# SEISMIC DAMAGE MECHANISM AND ENERGY DISSIPATION OF LONG-SPAN CABLE-STAYED BRIDGES


**Presented by Jianzhong Li**

**Tongji University**


**Oct.2, 2019**

# Outlines

1. Introduction

2 Seismic failure model of a long span cable-stayed bridge

3 Energy dissipation for a long span cable-stayed bridge

4 Conclusion

# 1. Introduction

- Many long span bridges such as Sutong Changjiang Highway Bridge (cable-stayed bridge with a main span of 1088m), Taizhou Changjiang Highway Bridge (a three-tower and two-span suspension bridge with two main spans of 1080 m), were built in China during the past two decades.

- More long-span bridges will continue to be constructed in China in the future. The Hutong Bridge for both railway and highway traffic (central span: 1092 m, double deck) , the Yangsigang Bridge (suspension bridge， central span: 1700m, double deck) are now under construction.

# 1. Introduction

## Top-five Long Span Bridges in Each Type in China

| Bridge Type | No | Name | Location | Girder type | Main Span [m] | Completion year |
|---|---|---|---|---|---|---|
| Suspension | 1 | Yangsigang | Hubei | Truss | 1700 | Under construction |
| | 2 | Xihoumen | Zhejiang | Twin steel box | 1650 | 2007 |
| | 3 | Runyang | Jiangsu | Steel box | 1490 | 2005 |
| | 4 | Taizhou | Jiangsu | Steel box | 1080 (three-tower) | 2012 |
| | 5 | Maanshan | Anhui | Steel box | 1080 (three-tower) | 2013 |
| Cable-stayed | 1 | Hutong | Jiangsu | Truss | 1092 | Under construction |
| | 2 | Sutong | Jiangsu | Steel box | 1088 | 2007 |
| | 3 | Edong | Hubei | Hybrid box | 926 | 2010 |
| | 4 | Jiujiang | Jiangxi | Steel box | 818 | 2013 |
| | 5 | Jinyue | Hubei | Steel box | 818 | 2010 |
| Arch | 1 | Chaotianmen | Chongqing | Truss | 552 | 2009 |
| | 2 | Lupu | Shanghai | Steel box | 550 | 2003 |
| | 3 | Bosideng | Sichuan | CFST | 518 | 2012 |
| | 4 | Wushan | Chongqing | CFSt | 460 | 2005 |
| | 5 | Mingzhou | Zhejiang | Steel box | 450 | 2011 |

# 1. Introduction

## ❖ Cable Stayed Bridge

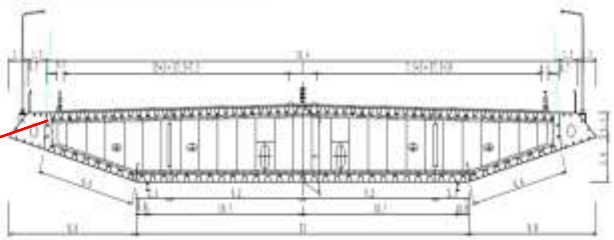

***Sutong Bridge***

**Span: 200+300+1088+300+200m**

**Completion year:  2008**

**It was the world's longest cable stayed bridge  until  2012.**

# 1. Introduction

## ❖ Cable Stayed Bridge under Construction

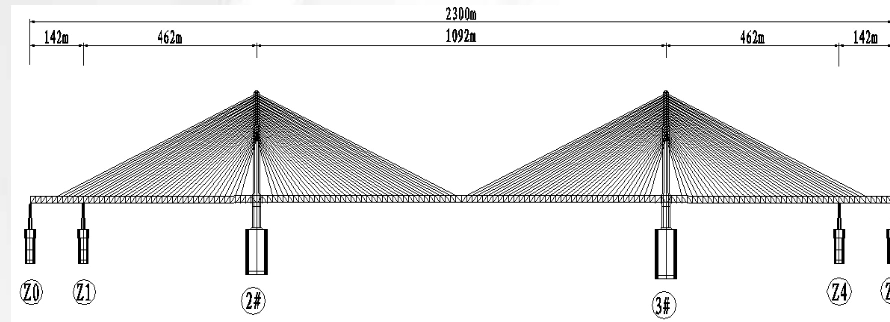


*Hutong Bridge*

Span:142m+ 462m +1092m+ 462m+142m

Bridge deck: steel truss girder ,16Hx35W

Estimated completion year: 2020

# 1. Introduction

- Meanwhile,  in recent year several major earthquakes occurred in world, such as  as the Chi-chi earthquake (1999). Wenchuan earthquake (2008),  Yushu earthquake (2010) and Kobe  earthquake (1995).  These earthquakes results many bridge damage.

Wenchuan Earthquake

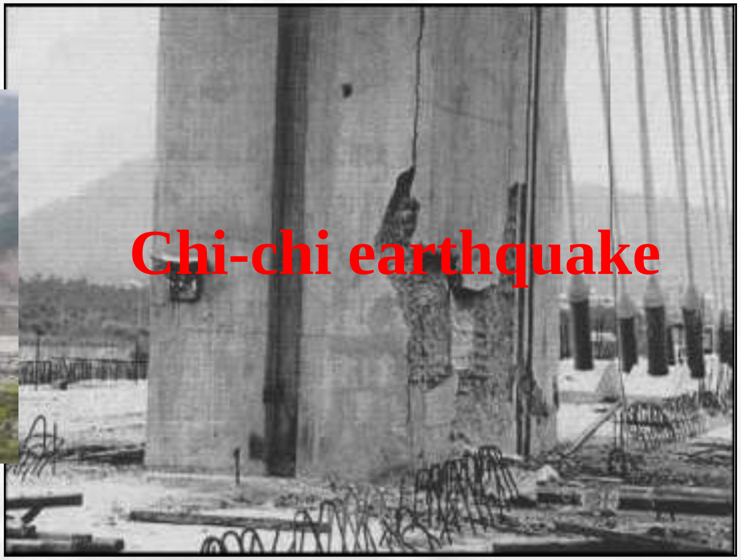

Chi-chi earthquake

# 1. Introduction

Wenchuan Earthquake

阪神地震

- The seismic performance of long span bridge have been attracted great attention in both bridge engineering and earthquake engineering

## 2 Seismic failure model of a long span cable-stayed bridge

- Based on a long-span cable-stayed bridge with a main span of 1088 m and typical inverted-Y-shaped towers.

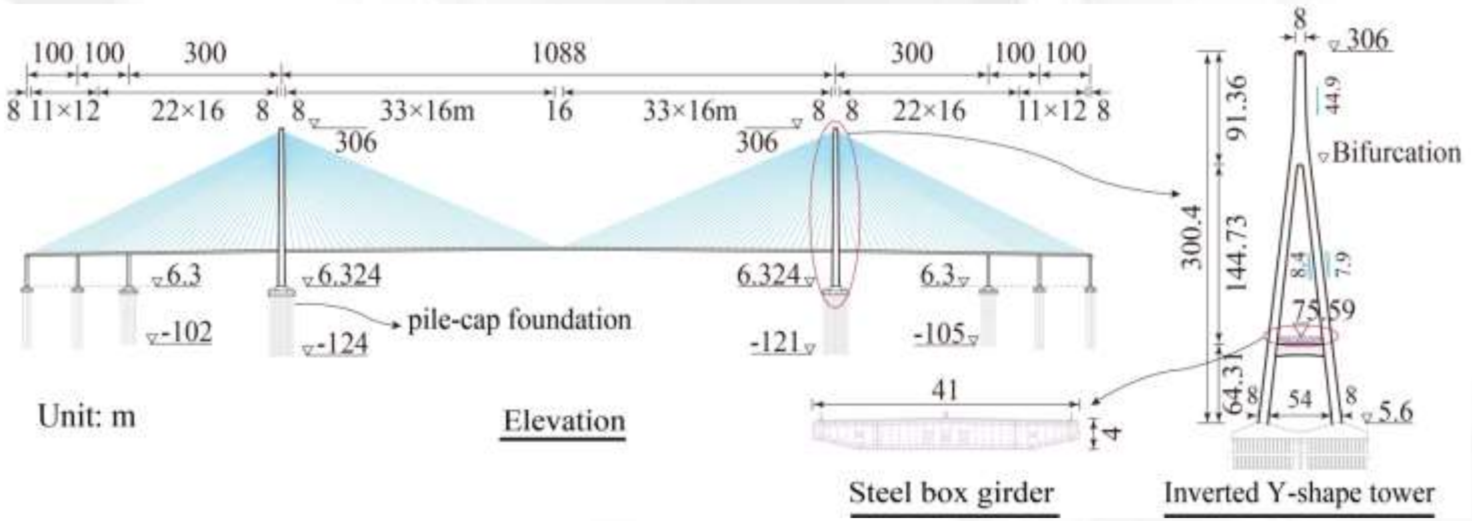


Configuration of Sutong Bridge

- The numerical analyses, quasi-static model tests and shake table model test are conducted to investigate the seismic damage mechanism and failure model

# 2 Seismic failure model of a long span cable-stayed bridge

## 2.1 numerical analyses for failure mechanism assessment

- A three-dimensional FE model of the Sutong Bridge is built in OpenSees. Plasticity-distributed fiber models are used to represent pylon sections accounting for material nonlinearity and axial force-moment interaction.
- Based on the site condition of Sutong Bridge , twelve non-pulse-like ground motion records are selected from PEER-NGA strong motion. IDA is conducted to assess failure model.

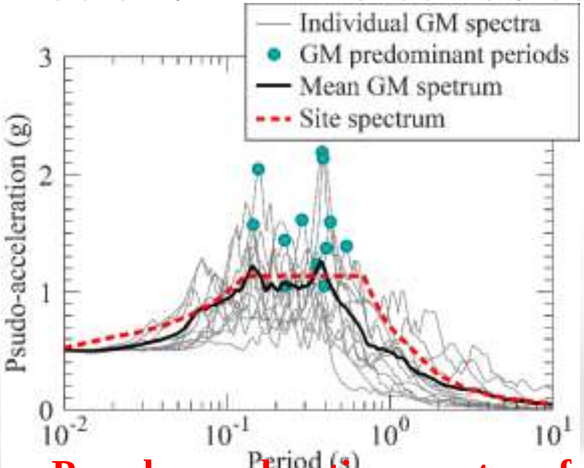


Pseudo-acceleration spectra of the adopted ground motion

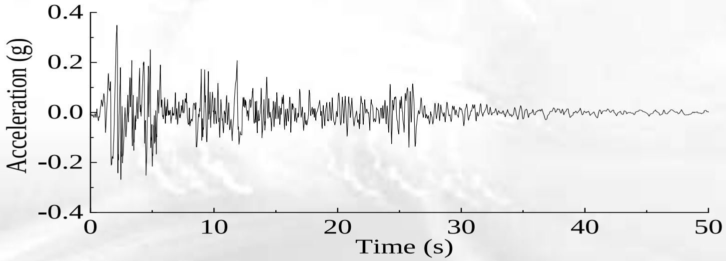

# 2 Seismic failure model of a long span cable-stayed bridge

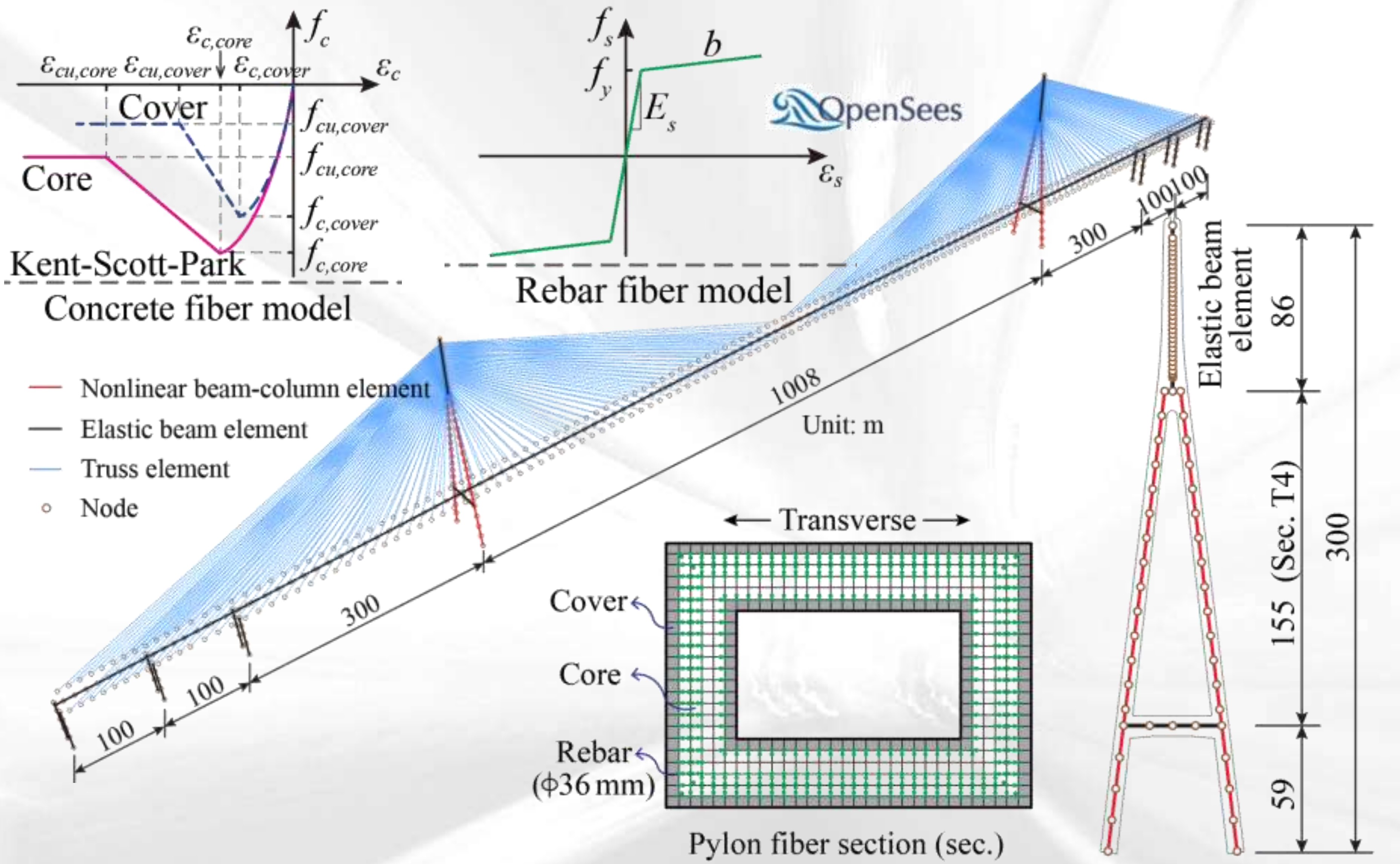

# 2 Seismic failure model of a long span cable-stayed bridge

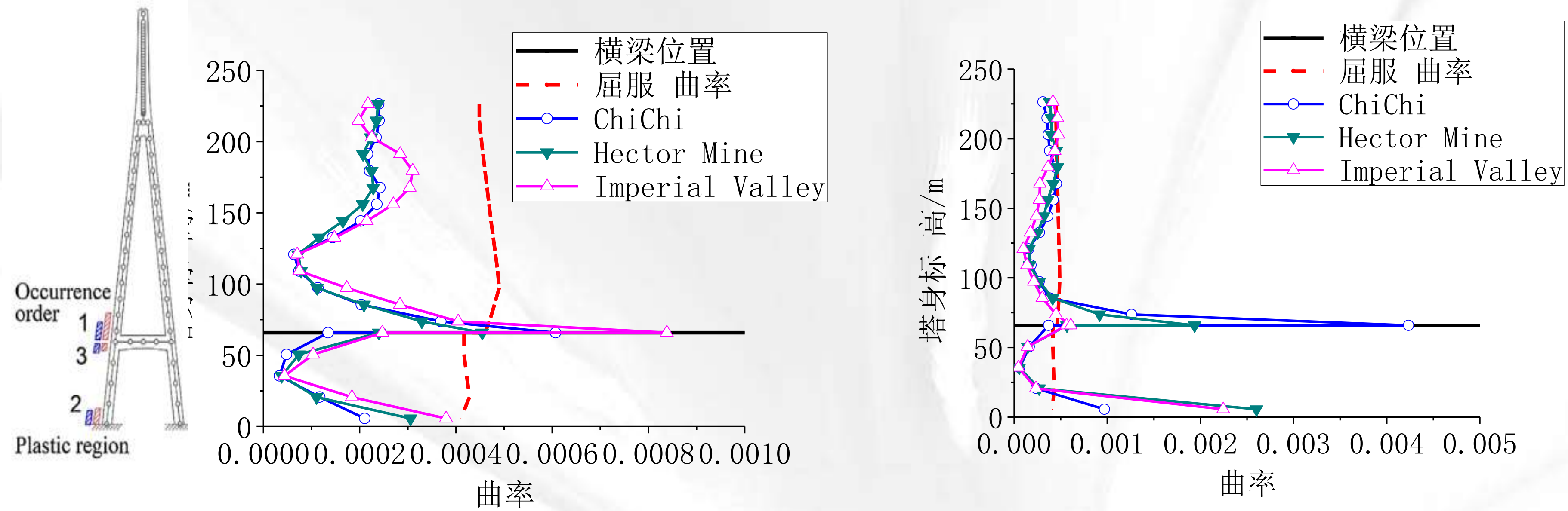


(a) curvature disturbance along the height at yielding state

(b) curvature disturbance along the height at ultimate state

- Plastic regions were observed at bottoms of the upper and lower columns as well as the top of lower column with concrete reach the ultimate stain at the bottom of upper column.

# 2 Seismic failure model of a long span cable-stayed bridge

## 2.2 quasi-static model test of the pylon

- A single pylon form Sutong Bridge is selected as prototype pylon of quasi-static model .
- A simplified displacement-controlled two-node load-pattern, one at the bifurcation-node and the another at the crossbeam is get using numerical analyses.

H=7.41m

Scale factor： 1/35

# 2 Seismic failure model of a long span cable-stayed bridge

- A full bridge FE model is built and subjected to a series of ground motions using IDA.
- IDA-based development of displacement ratio between the bifurcation-node and crossbeam is proposed
- A displacement ratio of 5.0 is then adopted in the test

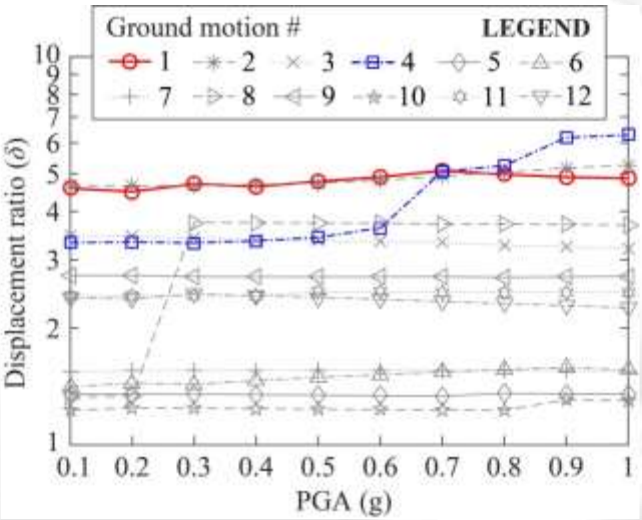


IDA-based development of displacement ratio between the bifurcation-node and crossbeam

# 2 Seismic failure model of a long span cable-stayed bridge

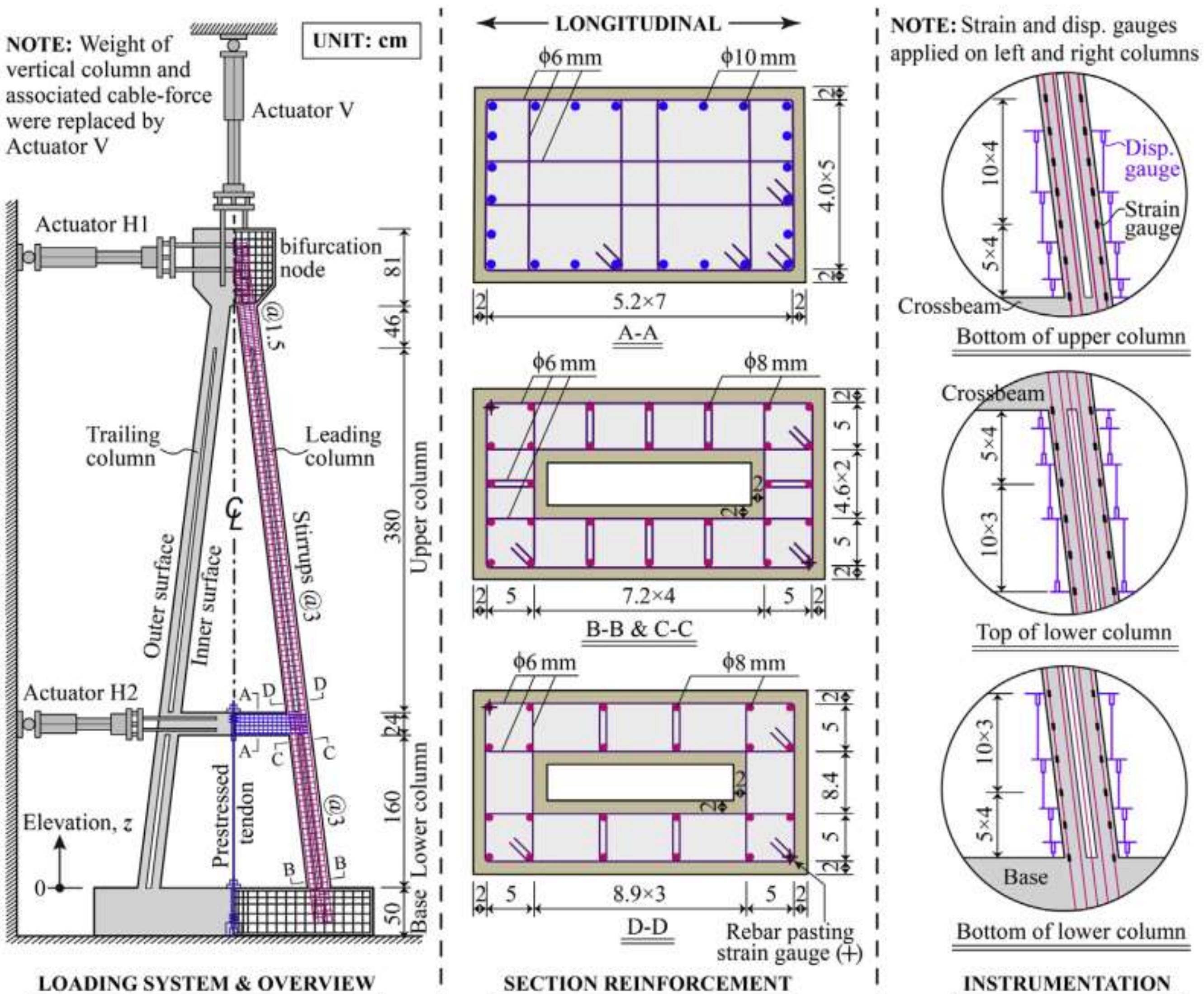


**Fig. 9.** Schematic of the quasi-static test: overview, reinforcement and instrumentation.

## 2 Seismic failure model of a long span cable-stayed bridge

### Test result discussion

#### ✓ Observed Damage

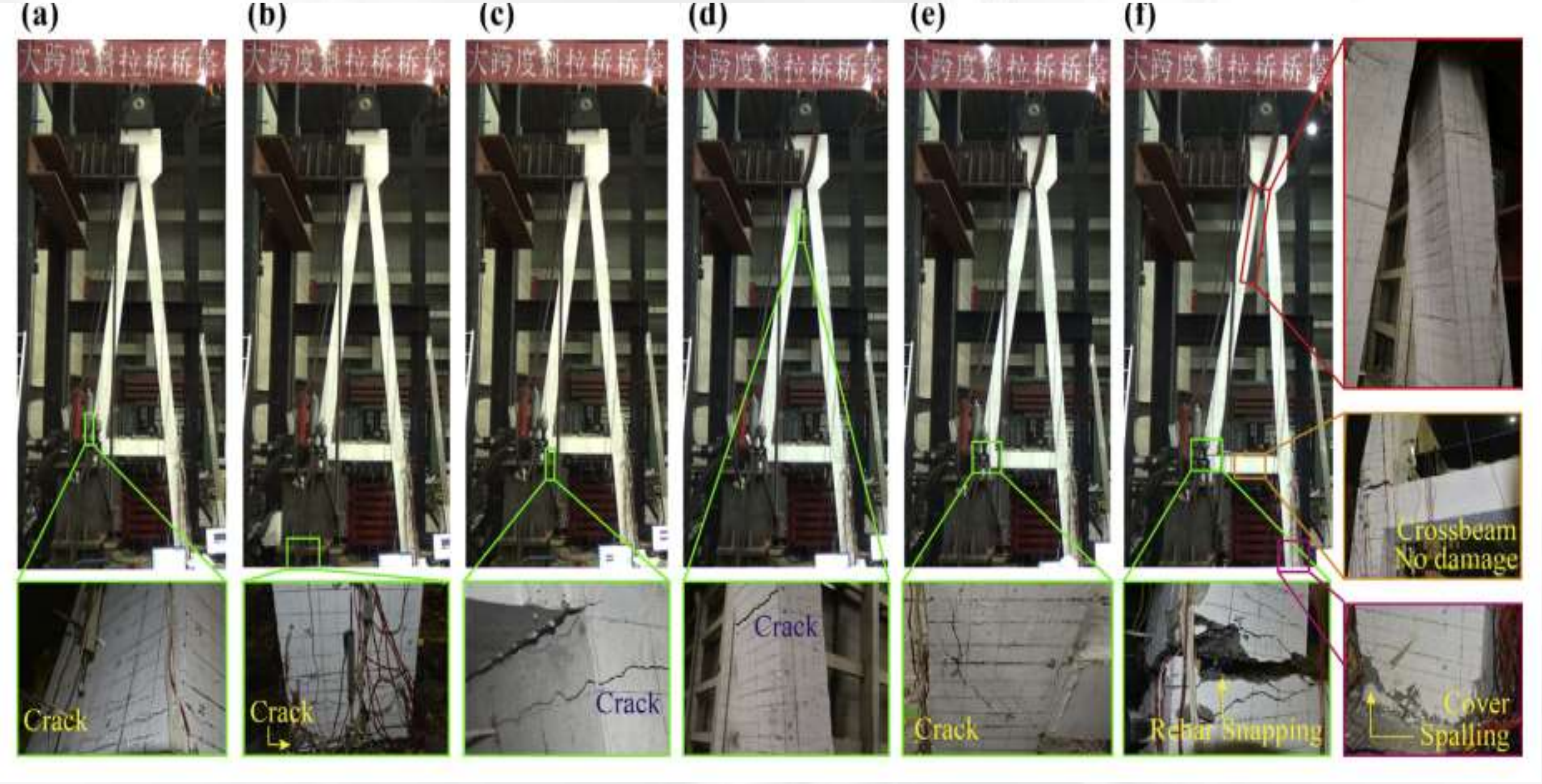


Development of the global deformation and corresponding local damage to the test model for increasing displacement levels at the bifurcation-node: (a) 25 mm; (b) 35 mm; (c) 45 mm; (d) 50 mm; (e) 140 mm; (f) 320 mm (ending displacement)

# 2 Seismic failure model of a long span cable-stayed bridge

| Table 7. Observed physical damage to pylon components during the test | | |
|---|---|---|
| **Disp.** | Description of observed damage | Figure |
| **25 mm** | Horizontal crack at the of the bottom of upper column | 14(a) |
| **35 mm** | Horizontal crack at the bottom of lower column | 14(b) |
| **45 mm** | Horizontal crack at the the top of lower column | 14(c) |
| **50 mm** | Horizontal crack at the top of upper column (just below the bifurcation-node) | 14(d) |
| **140 mm** | Diagonal crack at the transverse-parallel surface of column-crossbeam intersection | 14(e) |
| **220 mm** | Concrete cover began to spall at the bottom of lower column | / |
| **320 mm** | Rebar snapped at the bottom of upper column; Concrete cover spalling extended along the elevation. Test ended. | 14(f) |

## 2 Seismic failure model of a long span cable-stayed bridge

- ✓ **It is found that horizontal cracks are the most frequent damage in the test, indicating a flexural damage mode for the pylon model.**

- ✓ **Plastic regions  were observed at bottoms of the upper and lower columns as well as the top of lower column, which are generally consistent to the critical sections derived from the IDA results mentioned above**

# 2 Seismic failure model of a long span cable-stayed bridge

## ◻ Test and numerical analyses for failure mechanism assessment

- ✓ **A refined FE model for the test model is built, results from the test and numerical model, including force-displacement relationships, curvature and strain distributions, are compared to validate the refined FE model**

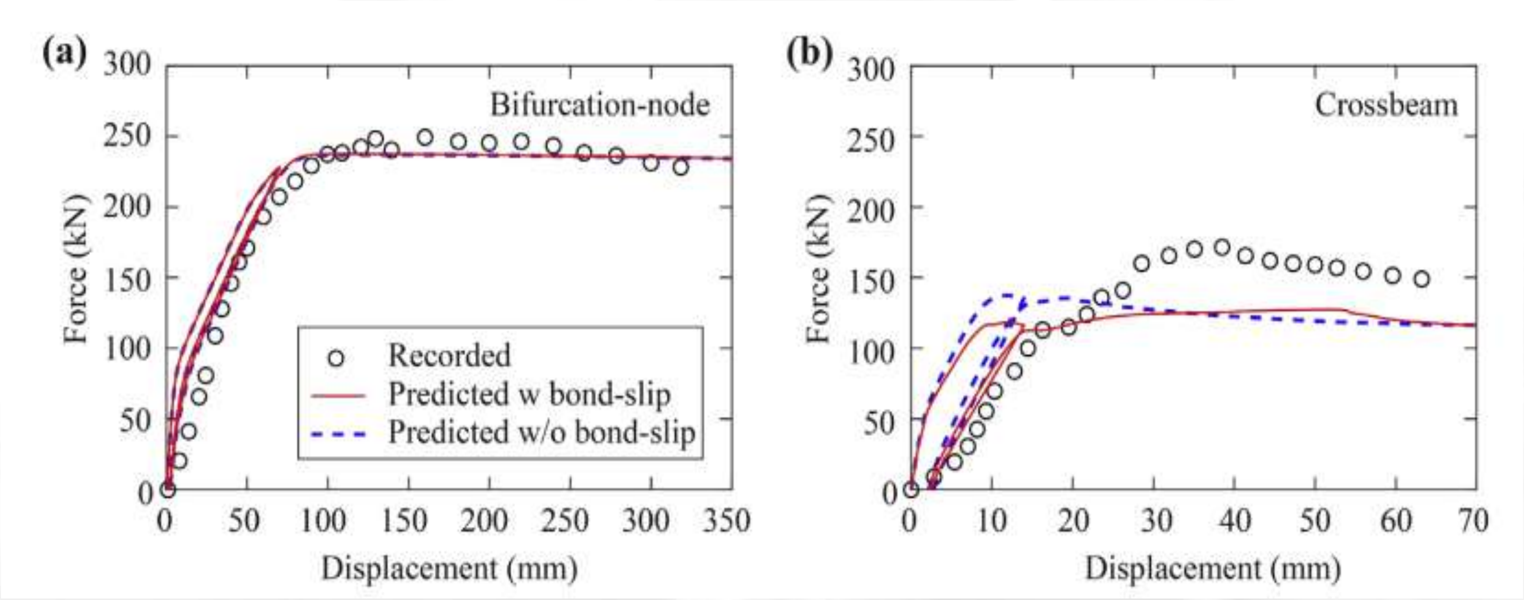


**Comparison of numerical results with the test results in terms of global force-displacement responses at two loading points: (a) bifurcation-node; and (b) crossbeam**

# 2 Seismic failure model of a long span cable-stayed bridge

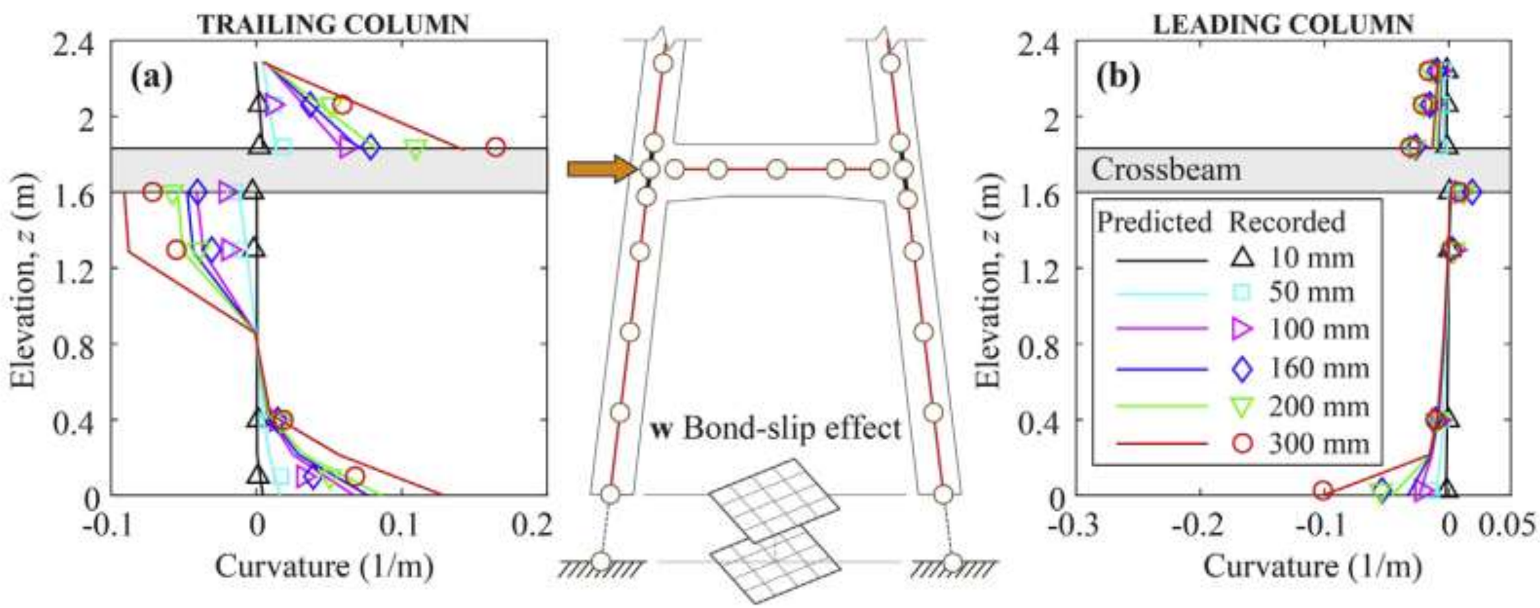


**Fig. 17. Comparison of numerical results with the test results in terms of curvature developments at increasing displacement levels at trailing and leading columns**

# 2 Seismic failure model of a long span cable-stayed bridge

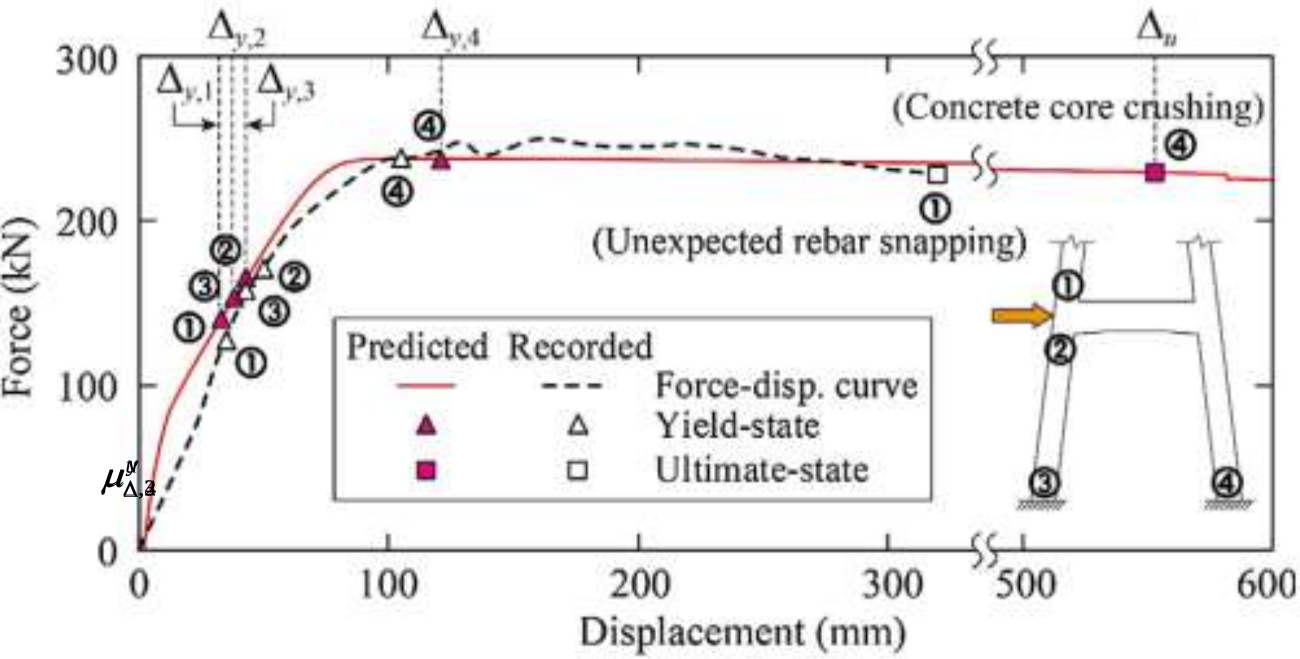


**Recorded and predicted failure process of the test model** [1.]

**Ductility factors for the second, third and fourth plastic hinges formed in the test.**

$$\mu_{\Delta,i}^{y} = \frac{\Delta_{y,i}}{\Delta_{y,1}}$$

**Ultimate displacement ductility factor**

$$\mu_{\Delta}^{u} = \frac{\Delta_{u}}{\Delta_{y,1}}$$

| | $\mu_{\Delta,2}^{y}$ | $\mu_{\Delta,3}^{y}$ | $\mu_{\Delta,4}^{y}$ | $\mu_{\Delta}^{u}$ |
|---|---|---|---|---|
| **Recorded** | 1.23 | 1.43 | 3.00 | 9.14 |

## 2 Seismic failure model of a long span cable-stayed bridge

- **The tested RC pylon model shows ductility factors of 1.23, 1.43 and 3.00 for the second, third and fourth plastic hinges formed in the test.**

- **the ultimate displacement ductility factor ($\mu_{\Delta}^{u}$) is relatively large values which indicate a flexural damage mode with considerable ductility .**

## 2.3 Shaking-Table Test Model of Long-Span Cable-Stayed Bridge

- A shaking-table experiment was conducted based on a long-span cable-stayed bridge with a main span of 1088 m and typical inverted-Y-shaped towers in order to investigated damage mechanism of a cable- stayed bridge under transverse earthquakes

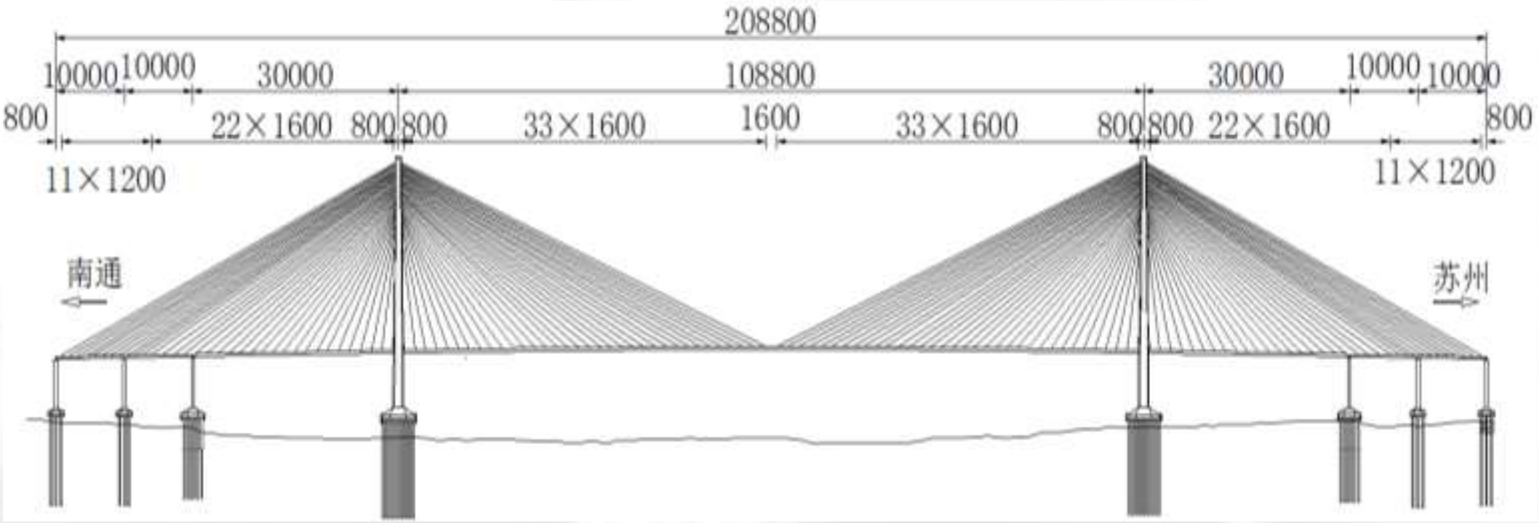


Figure 1 Overview of prototype bridge (Unit: m)

## 2 Seismic failure model of a long span cable-stayed bridge

### ◻ Shake Table *System Introduction*

- **The shake tables that have been used for model test is Multi-functional Shake Table System at Tongji University**
- **In the year of 2012, the Multi-functional Shake Table System at Tongji University was started to operate.**

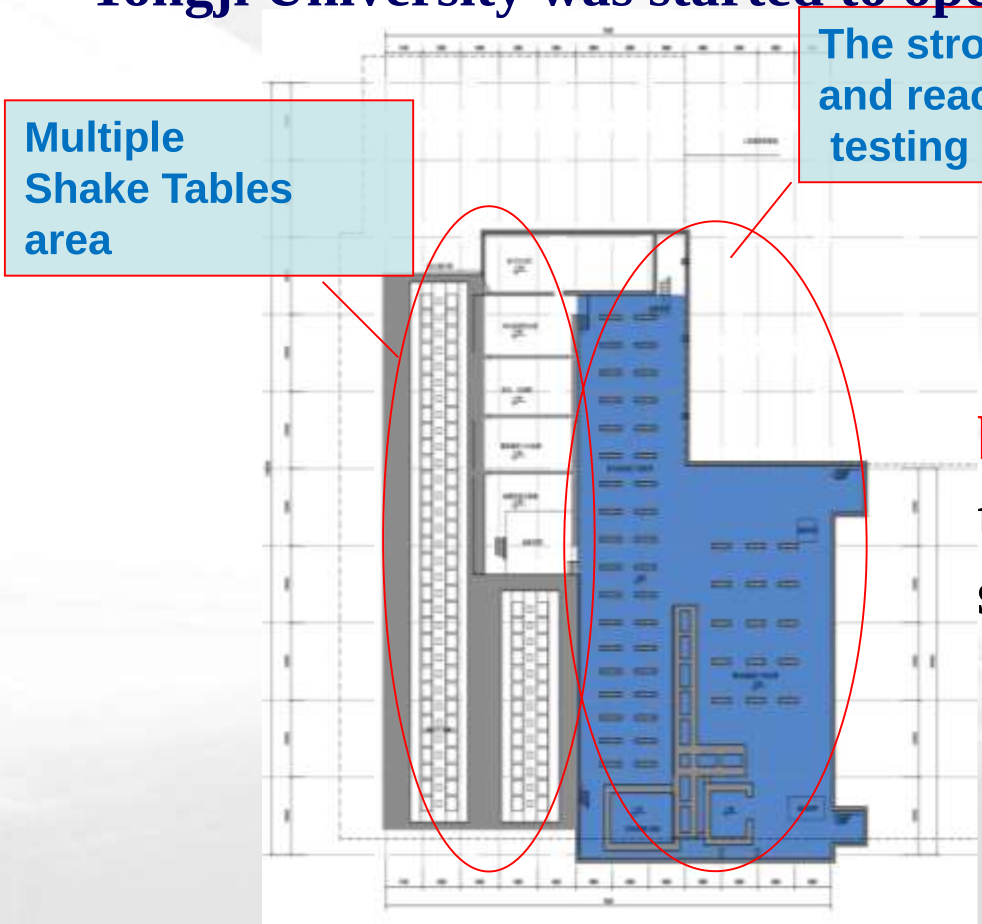


**14 different types of bridge models were tested by this system since its completion.**

## 2 Seismic failure model of a long span cable-stayed bridge

- The multiple shake tables system is composed of A(side table 30ton), B(main table 70ton), C(main table 70ton) and D(side table 30ton) 4 shake tables, each table has horizontal 3 D.O.F. (longitudinal, lateral, yaw) working modes.

# 2 Seismic failure model of a long span cable-stayed bridge

## Bridge model design

- **Geometric scale factor is 1/35， Acceleration scale factor is 1/1 and the total length of the model bridge reached to 59.65 m.**

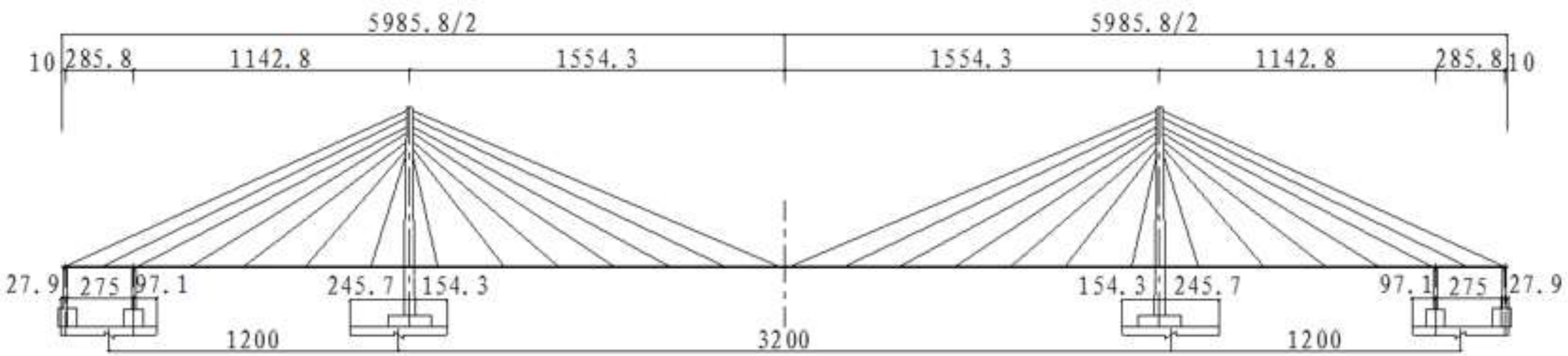


The Shake table test model

# 2 Seismic failure model of a long span cable-stayed bridge

- **Modeling of towers**
  - ✓ **Micro-concrete, which has approximately 30% of the strength and Young's modulus of prototype concrete, was used for the tower and bent of actual model**

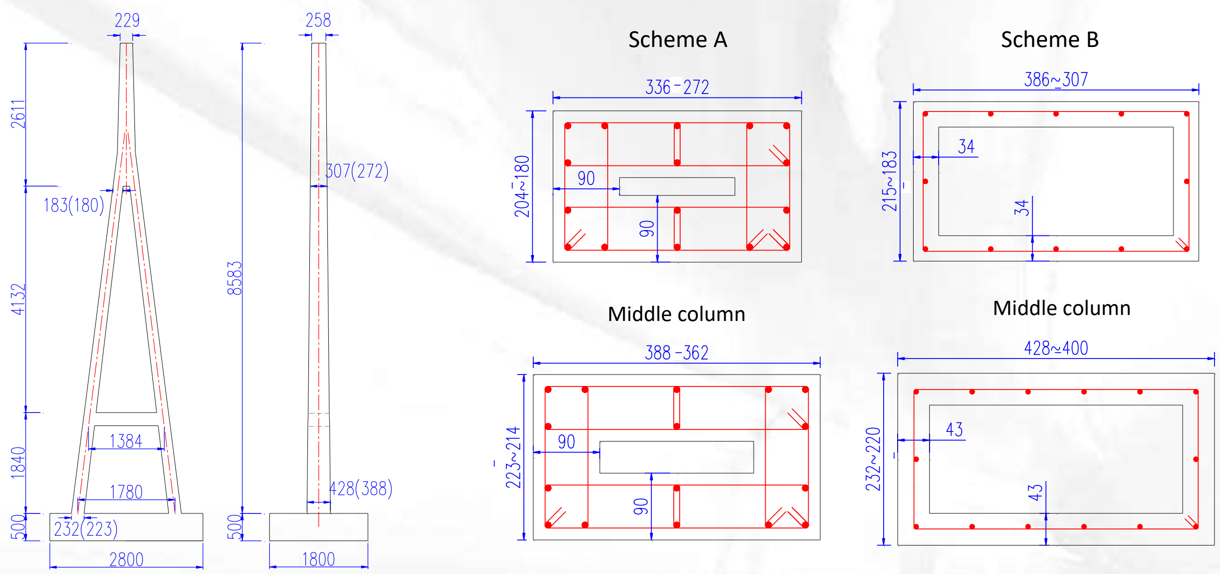


Note: Values in bracket are for Scheme A.

**Overview of model tower and section details (Unit: mm)**

# 2 Seismic failure model of a long span cable-stayed bridge

## Modeling of deck

- The model section was designed to have the required bending moments of inertia about both the strong and weak axes
- According to the scaling law. Additional rigid cross beams were used to provide the required anchoring locations of the cables to the deck.

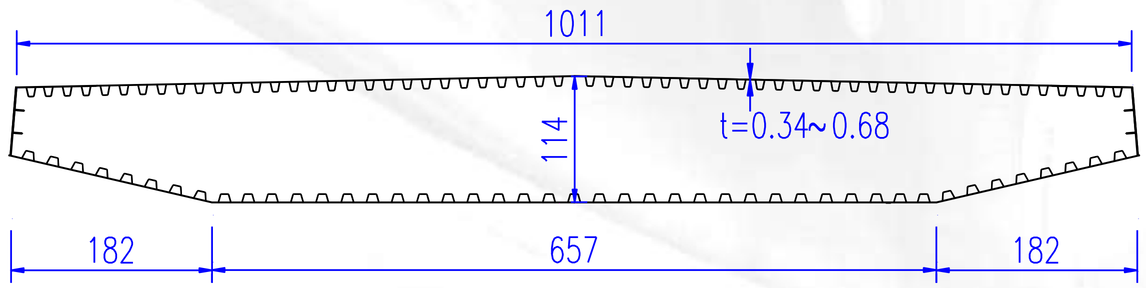


(a) Theoretically scaled girder section

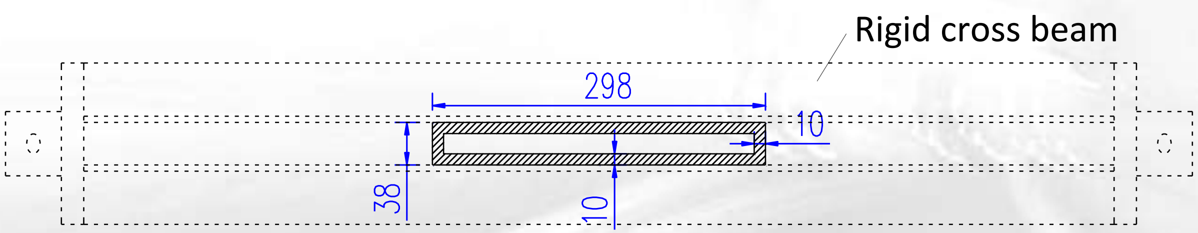


(b) Realistic girder section

**Section design of deck**

# 2 Seismic failure model of a long span cable-stayed bridge

- **Cable system, additional masses**
  - ✓ The prototype cable-stayed bridge has 136 pairs of cables.
  - ✓ The cable system of the bridge model was equivalent with 28 pairs of cables, each cable was modeled as a steel wire with 7.7 mm in diameter.

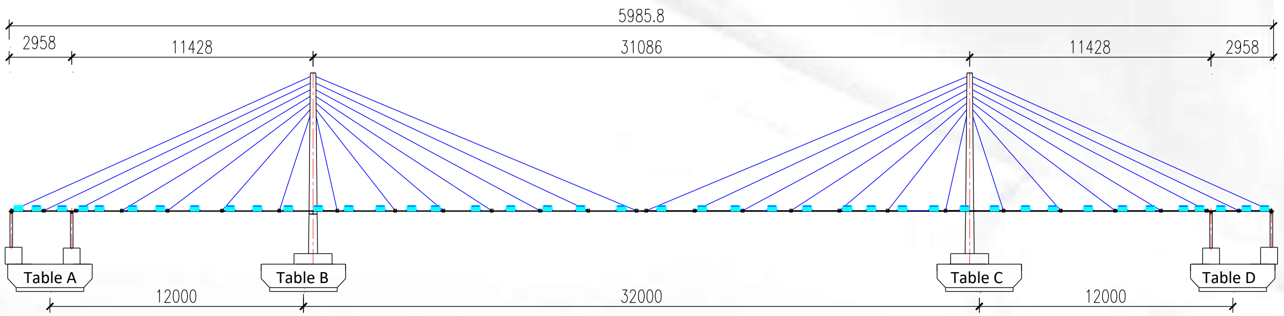



Cable system of the model bridge (unit: mm)

# 2 Seismic failure model of a long span cable-stayed bridge

- ✓ **Additional mass blocks are  provided an approximate mass distribution along the girder and the tower shafts according the similarity theory.**

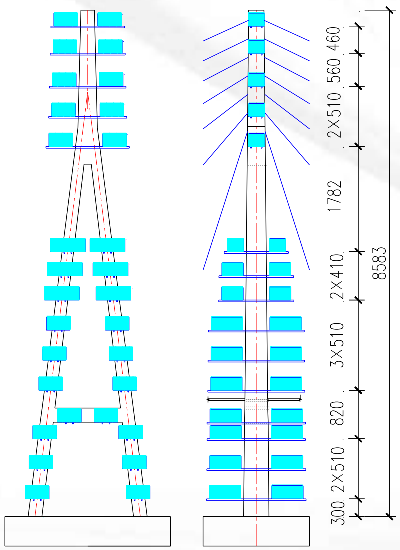


(b) Additional masses for towers

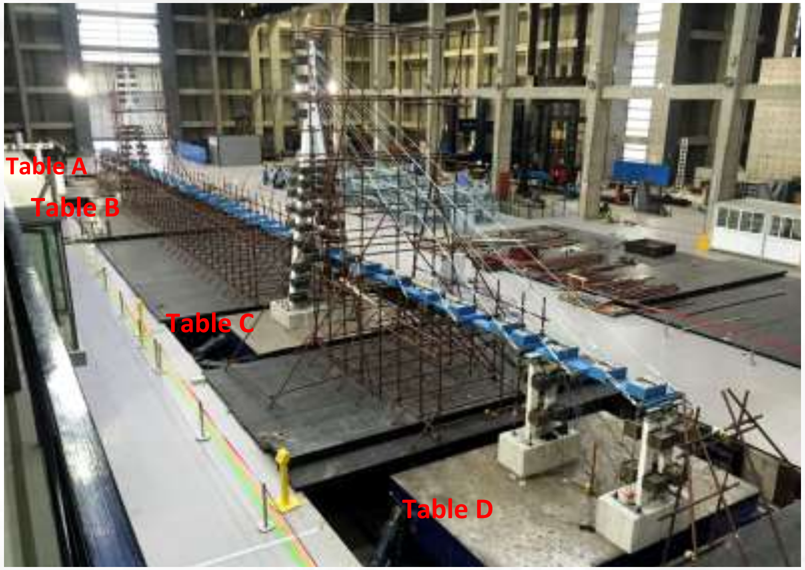


(c) Overview of model bridge

# 2 Seismic failure model of a long span cable-stayed bridge

## Earthquake input

- The aim of this test was to investigate the seismic responses and damage progression of the reinforced concrete towers with increasing excitation intensity.
- Site-specific seismic design ground motion with 2500-year return periods was as earthquake inputs.

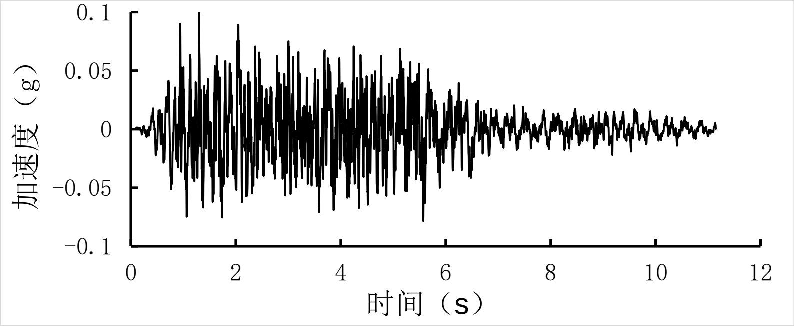


- The incremental PGA of the artificial ground motion was increased to investigate the damage progression of the towers with increasing PGA.

# 2 Seismic failure model of a long span cable-stayed bridge

Table 5 Test cases for damage progression of the towers

| Case | Input ground motion | PGA (g) |
|---|---|---|
| E1 | White noise | 0.1 |
| E2 | Artificial ground motion | 0.1 |
| E3 | Artificial ground motion | 0.2 |
| E4 | Artificial ground motion | 0.3 |
| E5 | Artificial ground motion | 0.4 |
| E6 | White noise | 0.1 |
| E7 | Artificial ground motion | 0.5 |
| E8 | White noise | 0.1 |
| E9 | Artificial ground motion | 0.7 |
| E10 | White noise | 0.1 |
| E11 | Artificial ground motion | 0.9 |
| E12 | White noise | 0.1 |
| E13 | Artificial ground motion | 1.1 |
| E14 | White noise | 0.1 |
| E15 | Artificial ground motion | 1.3 |

# 2 Seismic failure model of a long span cable-stayed bridge

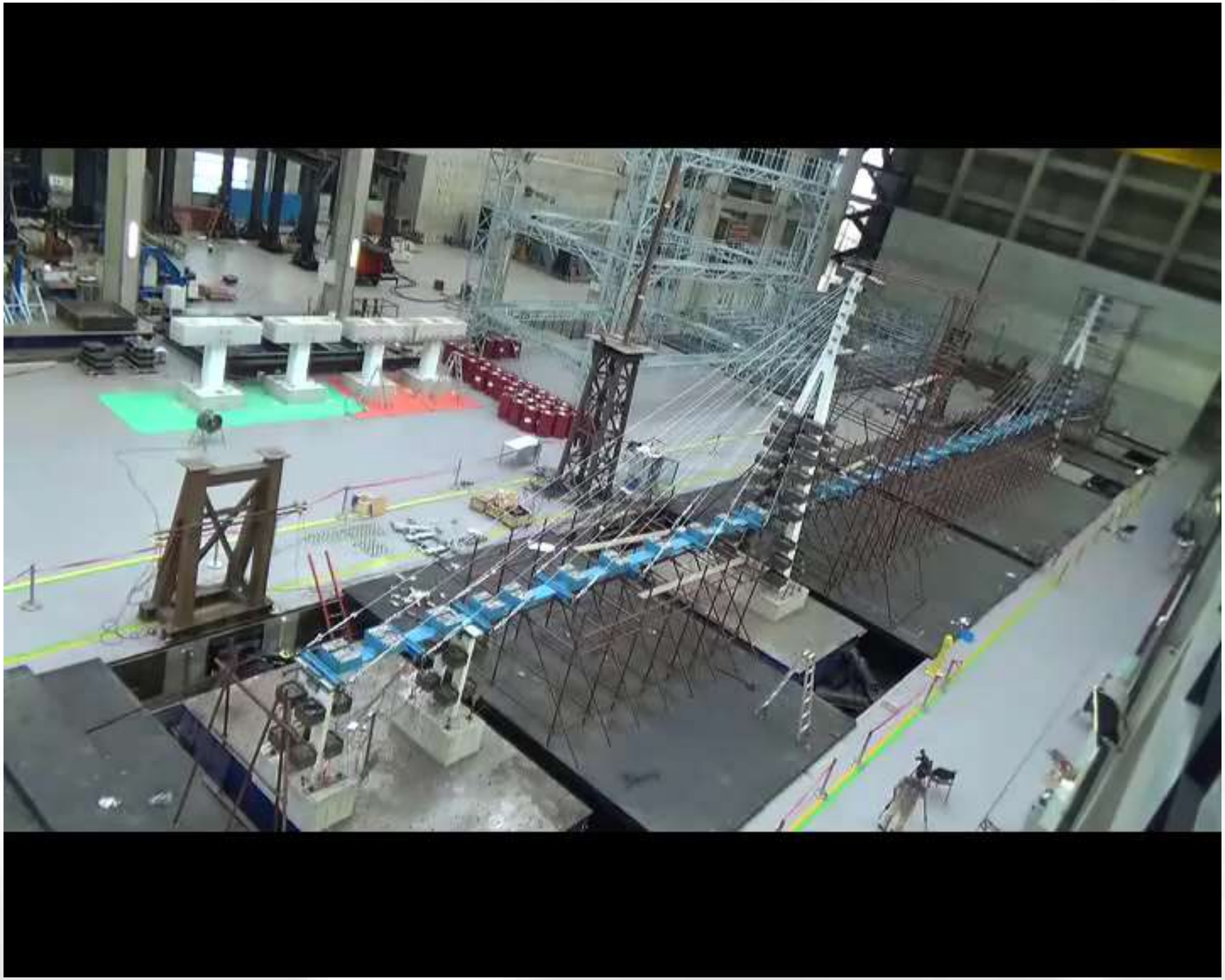

# 2 Seismic failure model of a long span cable-stayed bridge

# 2 Seismic failure model of a long span cable-stayed bridge

## Observed damage

- ✓ Visible residual cracks initially occurred in the upper tower columns, at approximately 10 cm to 15 cm from the base in test case E7 (PGA = 0.5 g) (Figure 17a).

- ✓ With an increase in the input PGA, the crack width slightly increased and more cracks were formed in the upper tower columns (Figures 17a and 17b).

- ✓ Visible residual cracks in the lower tower columns were firstly observed in test case E11 (i.e., PGA = 0.9 g).

- ✓ When the PGA of the ground motion was increased to 1.1 g, evident concrete spalling was observed in upper tower at approximately 20 cm to 25 cm from the base .

# 2 Seismic failure model of a long span cable-stayed bridge

- ✓ **During the running of case E15 (i.e., PGA = 1.3 g), a sudden failure occurred in the right upper tower column of the north tower (Figure 17e) and caused significant tilt of the tower (Figure 17f).**

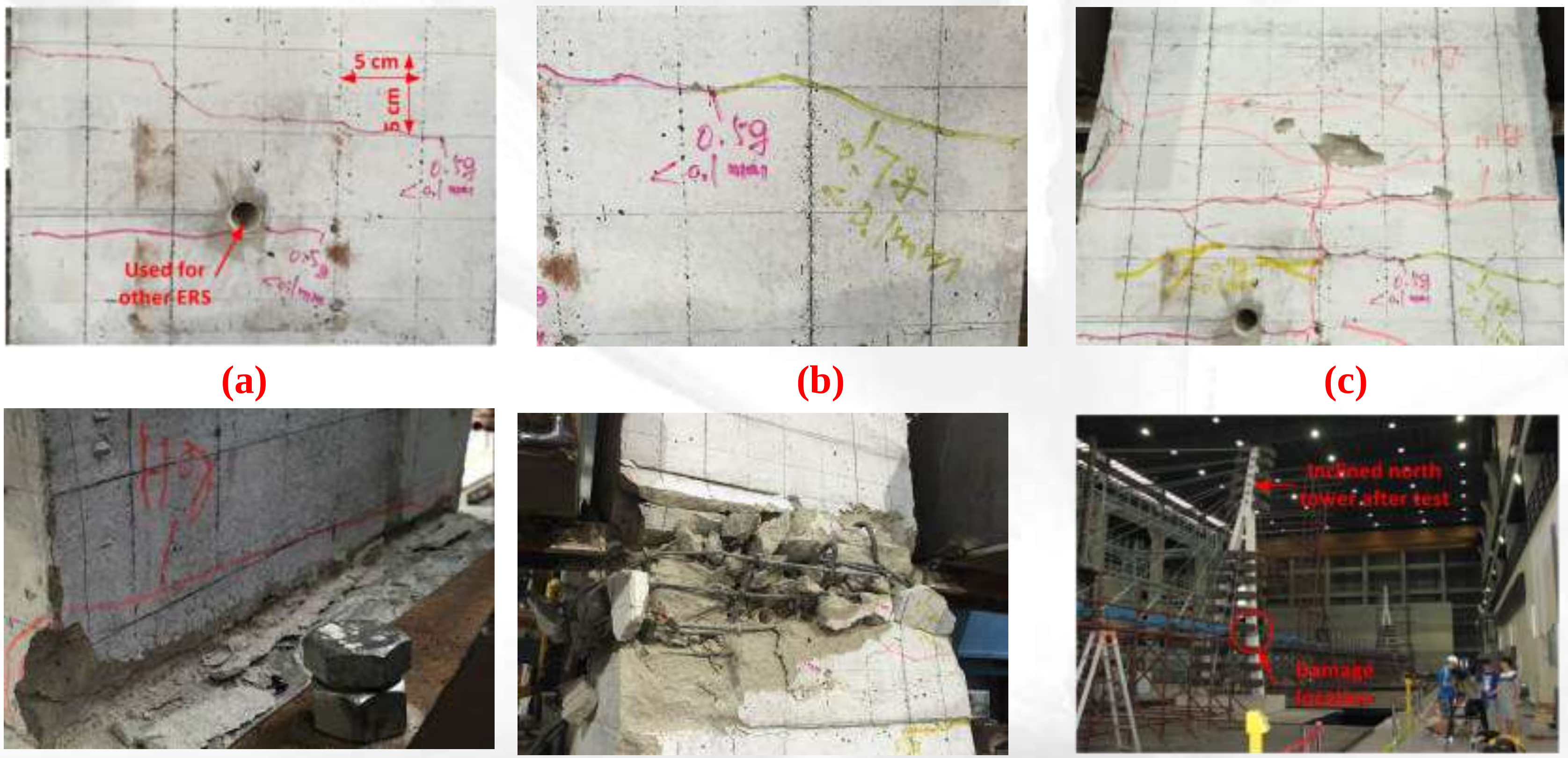


(a) (b) (c)

(d) (e) (f)

**Figure 17 Observed damage of bridge model**

# 2 Seismic failure model of a long span cable-stayed bridge

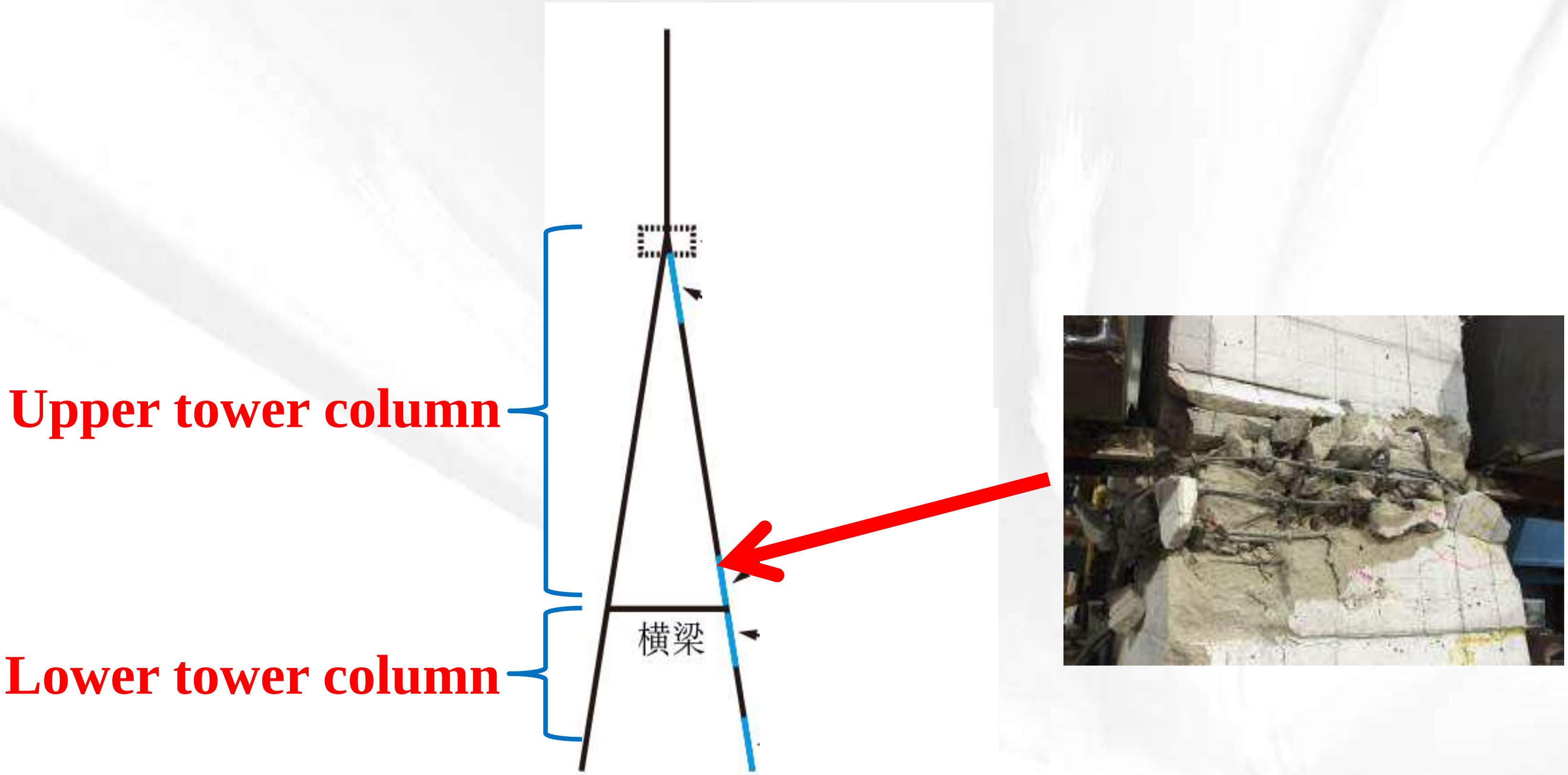


**Note that the failure mode was quite consistent with the numerical simulation and quasi-static model test of the pylon**

# 2 Seismic failure model of a long span cable-stayed bridge

## Test results analyses

- ✓ **The displacement of the tower increase as the PGA.**

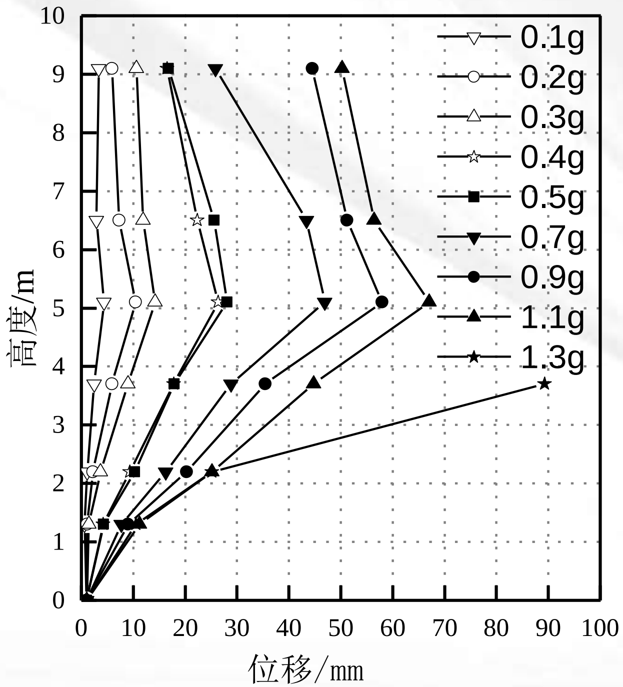


The envelopes of the displacement profileof the tower columns from the experimental data

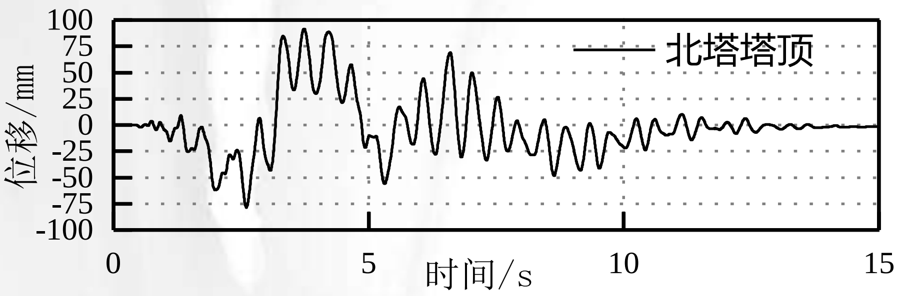


Displacement time histories at tower top

（PGA=1.1g）

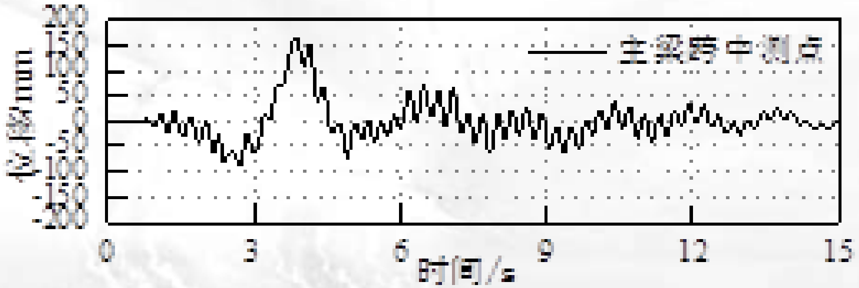


Displacement time histories at the mid-span of the girder

（PGA=1.1g）

# 2 Seismic failure model of a long span cable-stayed bridge

(a) Displacement time histories

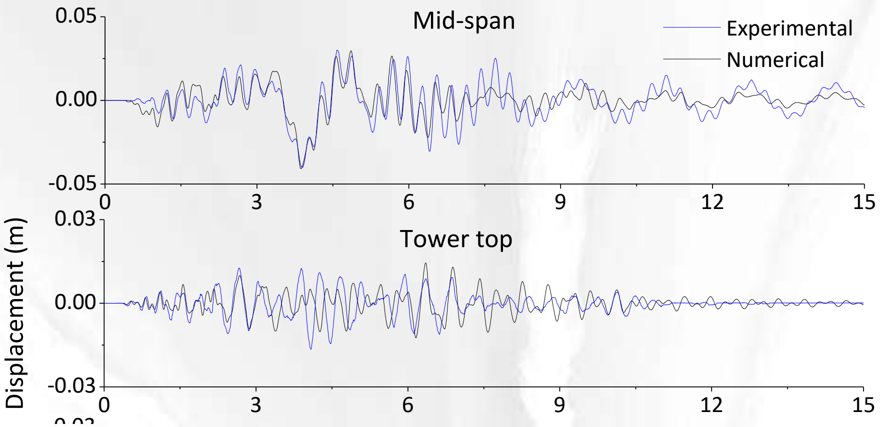


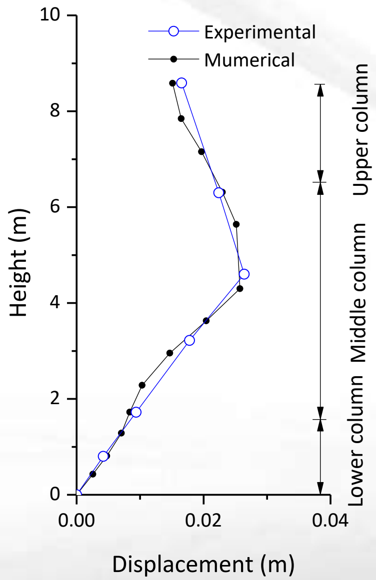


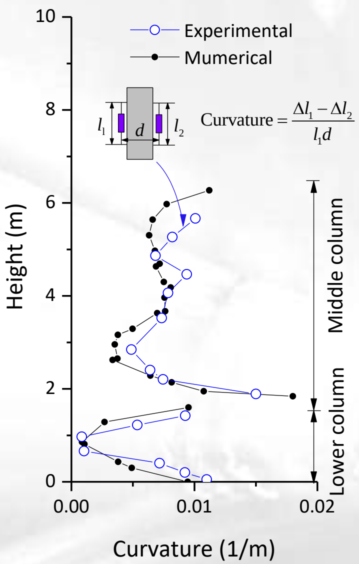


(b) Envelop of displacement (c) Envelop of curvature

Figure 18 Comparison of numerical and experimental responses for case E7 (i.e., PGA = 0.5 g)

# 3 Energy dissipation for of long span cable-stayed bridges

- **There are two main types of damper have been widely** applied to long-span bridges to mitigate the seismic response of the structure in China

  - **One is** Viscous Fluid Damper(VFD), which is velocity-dependent .

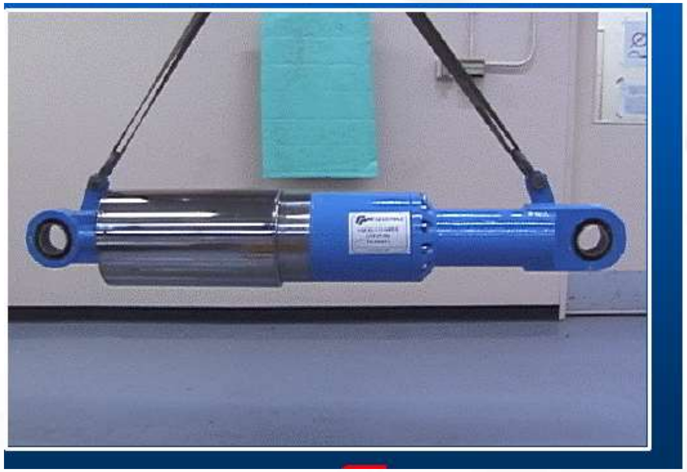

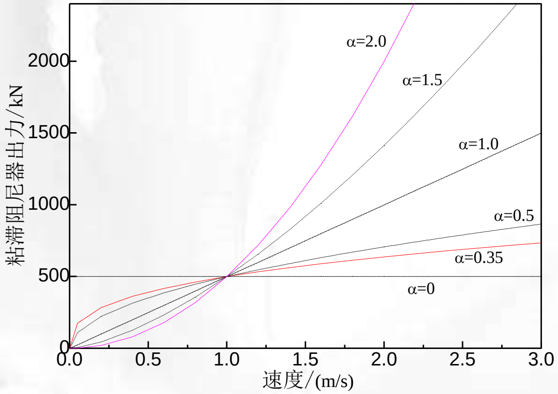


$$F = CV^{\alpha}$$

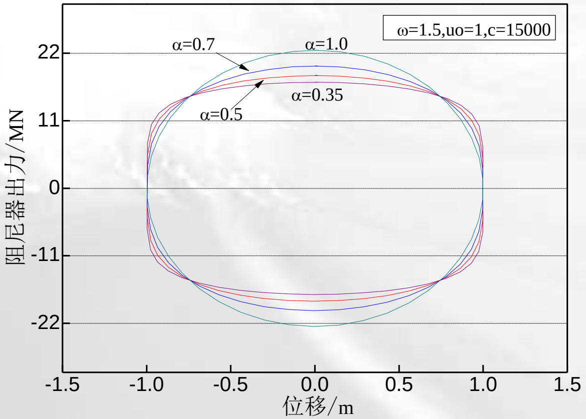

# 3 Energy dissipation for of long span cable-stayed bridges

- **The another is Elasto-plastic dampers :** a displacement-dependent damping device.

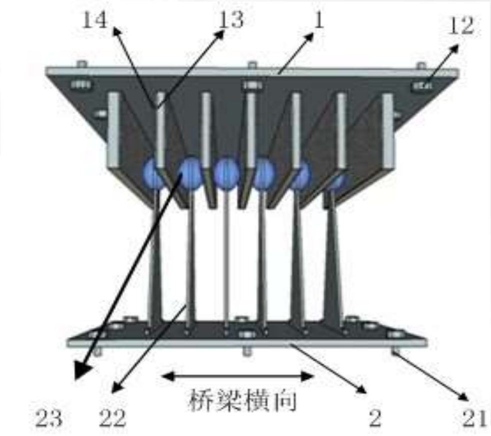


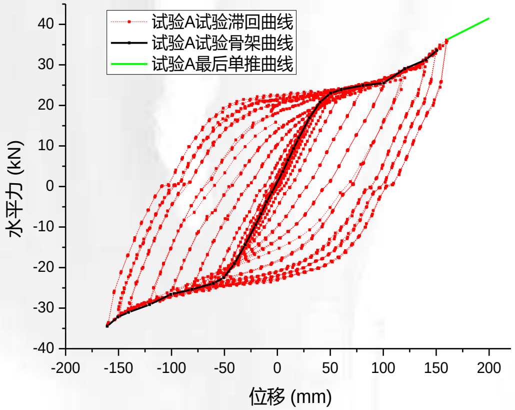


**a) Triangular-Shaped Metallic Dampers(TSD)**

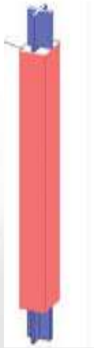

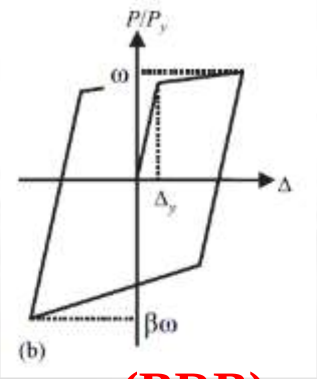


**b) Buckling Restrained Braces (BRB)**

# 3 Energy dissipation for of long span cable-stayed bridges

- **Before the final experimental test on the damage progression of the cable-stayed bridge, other tests on the model with FVDs and ) Triangular-Shaped Metallic Dampers(TSD) were carried out**

- **During these test cases, all structural members were required to behave elastically so that no damage would have occurred to the towers before the final test for the investigation of damage progression.**

# 3 Energy dissipation for of long span cable-stayed bridges

## 3.1 The effect  of Viscous Fluid Damper(VFD)

- In the longitudinal direction, the four prototype viscous dampers at each tower location were scaled into one model viscous damper

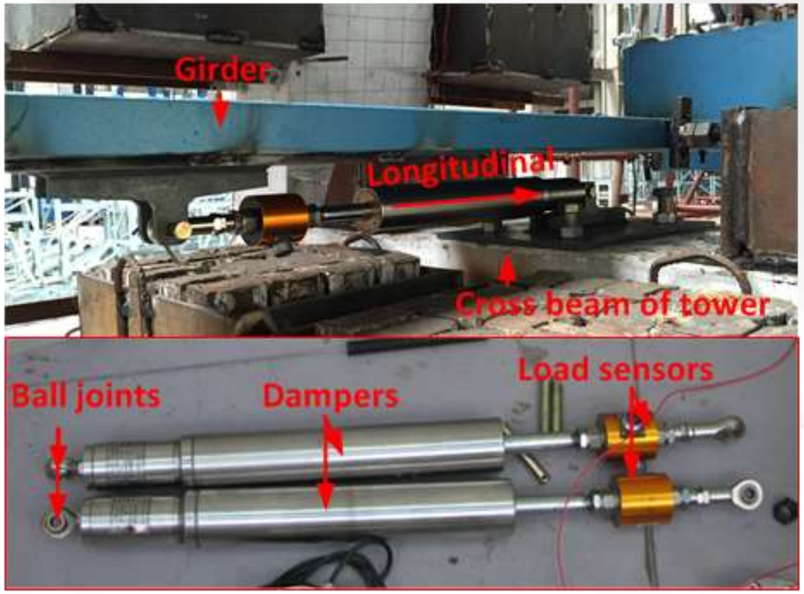


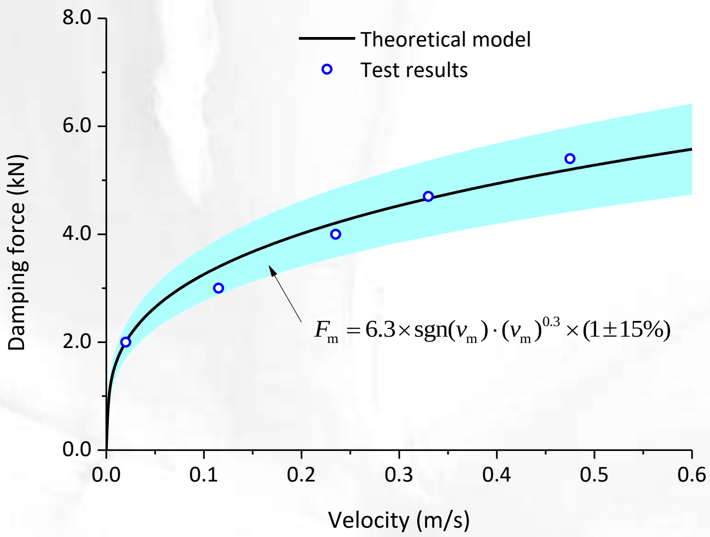


(a) View of configuration and installation (b) Force–velocity relationship

Figure  Design of viscous dampers and performance validation

- The damping coefficient of the model  damper was set to  6.5 $kN \cdot (s/m)^{0.3}$ based on the similarity theory.

# 3 Energy dissipation for of long span cable-stayed bridges

- **There were four ground motions adopted in this study as shown in table**

**Table 5.** Information of input ground motions

| No. | Earthquake, year | Station | Magnitude |
|---|---|---|---|
| 1 | Artifical | --- | --- |
| 2 | Chi-Chi. 1999 | HWA014, N | 7.62 |
| 3 | Loma Prieta, 1989 | Saratoga - W Valley Coll., 270 | 6.93 |
| 4 | El Centro, 1940 | El Centro Array #9, 180 | 6.95 |

- **The seismic effects of the structure under uniform excitation and un-uniform excitation (effects of wave passage) on the bridge with and without viscous dampers are investigated**

# 3 Energy dissipation for of long span cable-stayed bridges

## ◻ Uniform excitation

➢ Effects of **VFD on** displacements

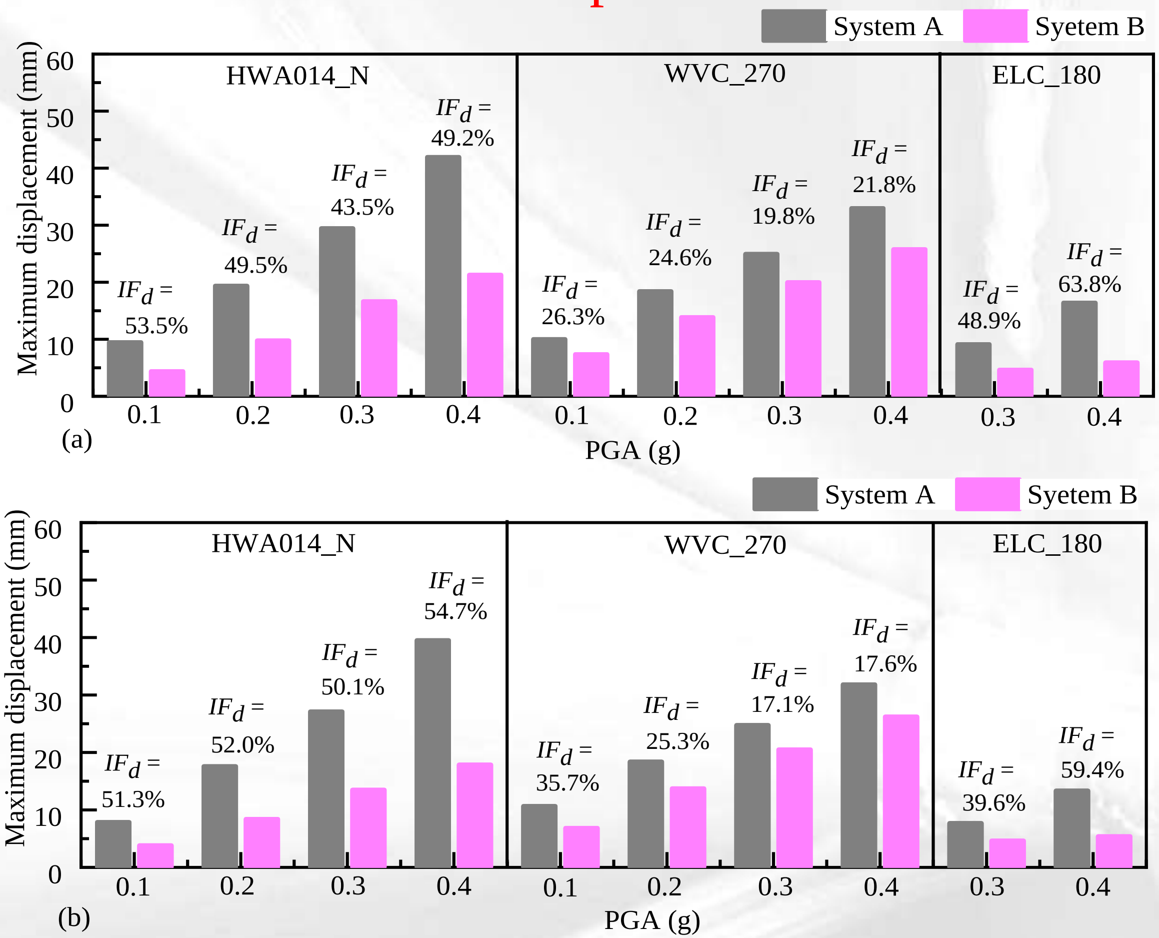


**Fig. 12.** Comparisons of the maximum displacements between System A and System B: (a) at tower top, **(b) at deck end**

✓ **The system A and system B are cable-stayed without and with VFD, respectively.**

# 3 Energy dissipation for of long span cable-stayed bridges

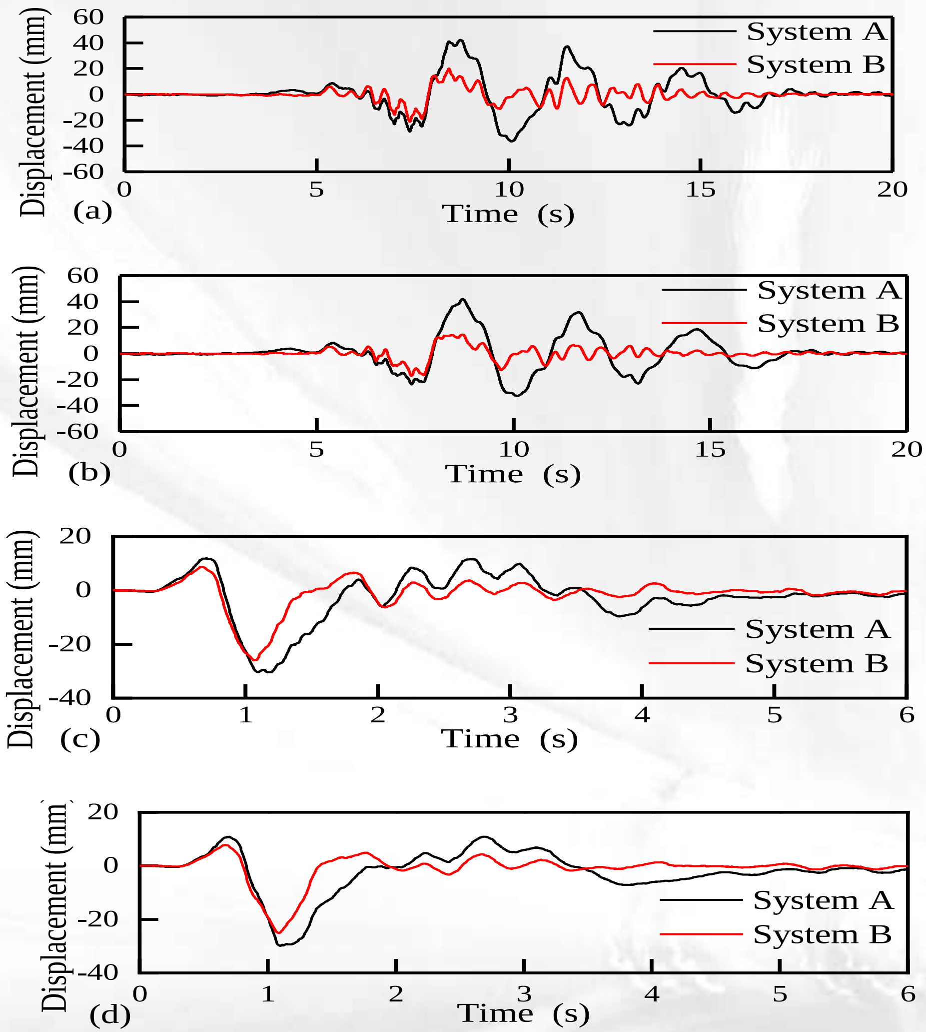


**Fig. 13.** Comparisons of displacement time histories between System A and System B (PGA=0.4g): (a) at tower top under Chi-chi earthquake, (b) at deck end under Chi-chi earthquake, (c) at tower top under Loma Prieta earthquake, (d) at deck end under Loma Prieta earthquake.

# 3 Energy dissipation for of long span cable-stayed bridges

- ✓ **The displacement at end of deck and at top of the tower in the longitudinal direction can be decreased effectively by using viscous dampers .**

- ✓ **However , different types of ground motions have significant influence on the mitigation effect of the viscous dampers to displacement responses. Velocity pulse of near-fault ground motion (Loma Prieta wave) led to low mitigation effectiveness.**

# 3 Energy dissipation for of long span cable-stayed bridges

➢ Effects of **VFD on** the strain of rebar

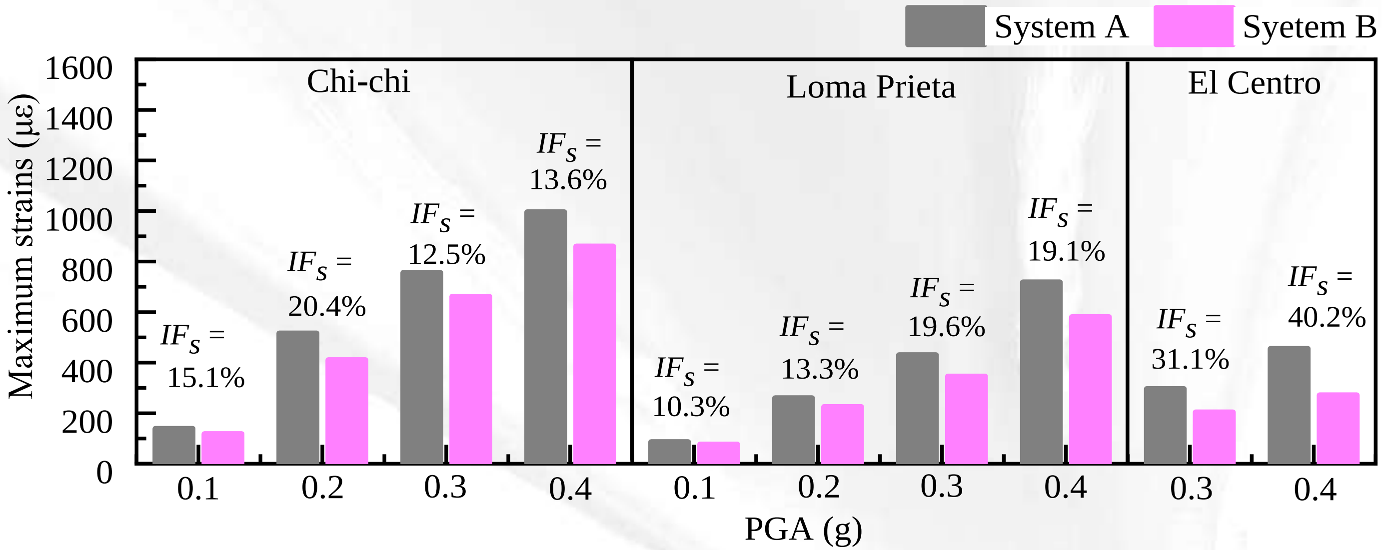


**Fig.** Comparisons of the maximum strains of longitudinal rebars at tower base between System A and B

✓ **The maximum strain of** rebars at tower base **could be reduced by VFD. The strains were reduced by 13.6%, 19.1%, and 40.2% under the Chi-chi, Loma Prieta and El Centro_180 waves at PGA of 0.4g, respectively.**

# 3 Energy dissipation for of long span cable-stayed bridges

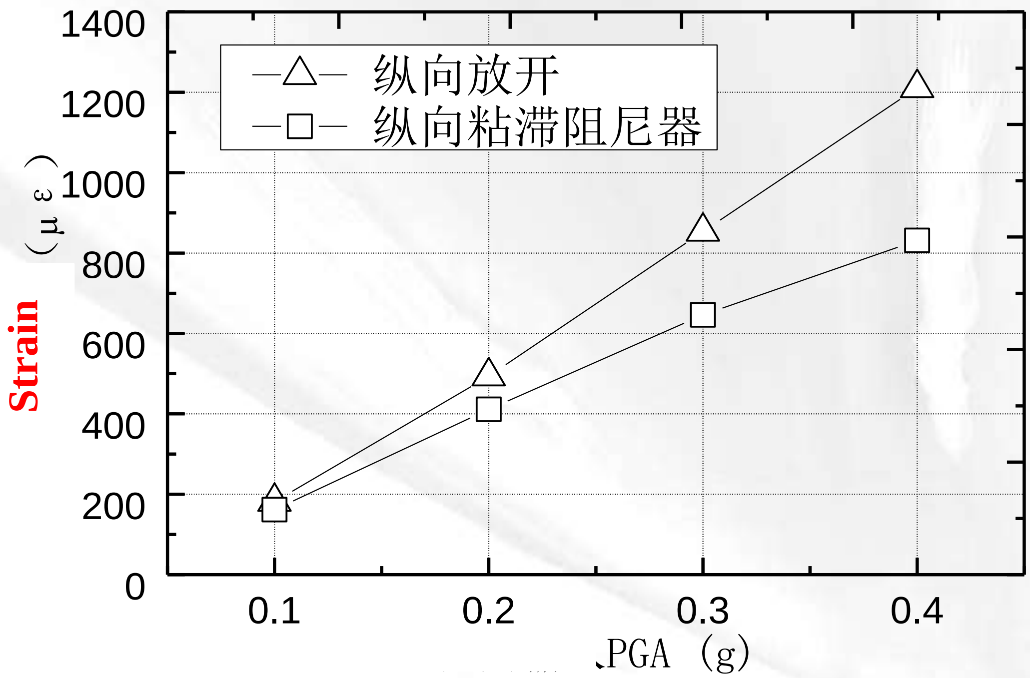


Strain of rebars at tower base with and without VFD

# 3 Energy dissipation for of long span cable-stayed bridges

## ➢Responses of viscous damper

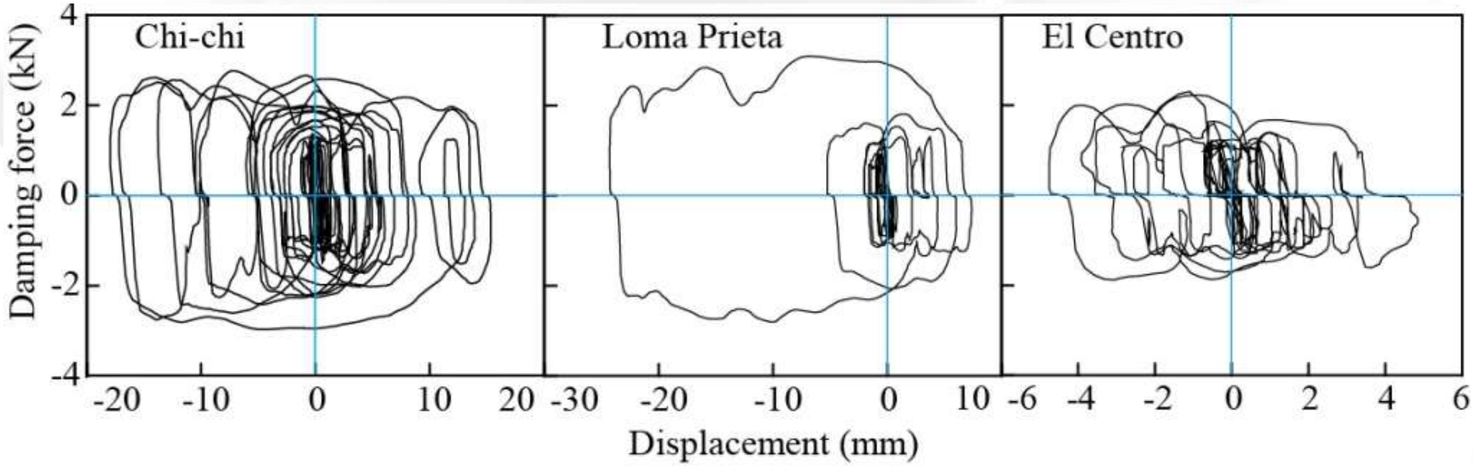


**Fig. Force-displacement hysteresis curves of viscous dampers under different earthquakes at a PGA of 0.4g.**

- ✓ **It should be noted that there was only one wide hysteresis curve observed under the Loma Prieta wave without consecutive and repeat energy dissipation as under the Chi-chi. This phenomenon is consistent with the low mitigation effect in displacement responses in System B previously.**

# 3 Energy dissipation for of long span cable-stayed bridges

## ☐ Wave passage effects

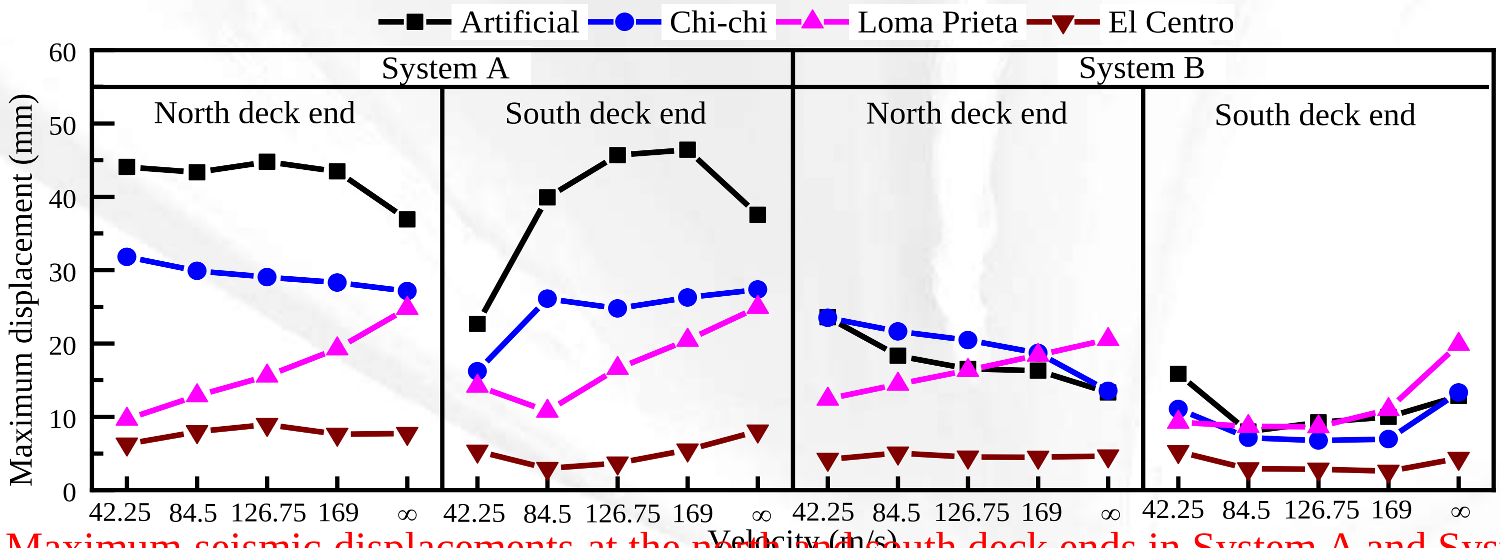


**Fig. 20.** Maximum seismic displacements at the north and south deck ends in System A and System B with different earthquake wave velocities.

- ✓ **Evident asynchronous responses can be commonly seen between the north and south deck end when considering wave passage effect**
- ✓ **Quite complicated variations of the displacement responses with the increasing of wave velocity were presented**

# 3 Energy dissipation for of long span cable-stayed bridges

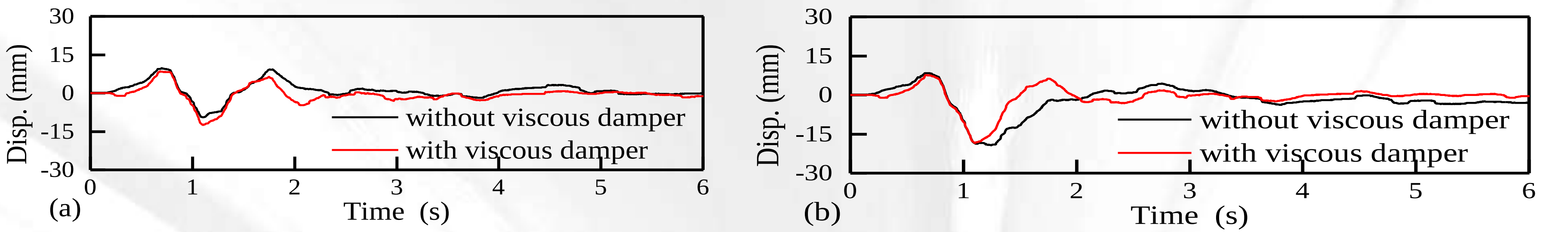


**Fig. 25.** Displacements time histories at north deck end under **the Loma Prieta wave** : (a) wave velocity = 42.25 m/s, (b) wave velocity = 169 m/s.

- ✓ **It can be seen that the displacement time histories with and without viscous dampers was quite similar and little mitigation effect can be seen from the additional viscous dampers**

- ✓ **This indicates that low or even negative mitigation effect might be induced by the additional viscous dampers under near-field ground motions when considering wave passage effect.**

# 3 Energy dissipation for of long span cable-stayed bridges

## 3.2 The effect of Elasto-plastic dampers (TSD) (transverse direction)

- In the transverse direction, the TSDs were placed at deck-tower and/or deck-bent connections to reduce seismic for bridge towers or bents

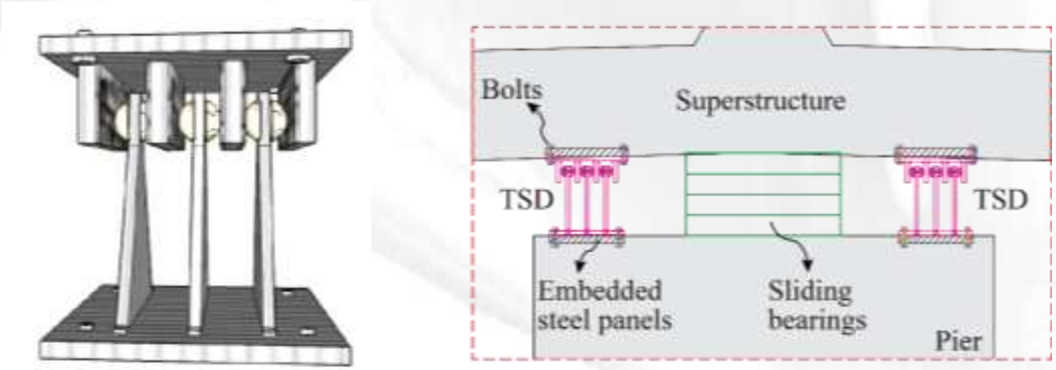


Configuration of TSDs

(a) Deformation

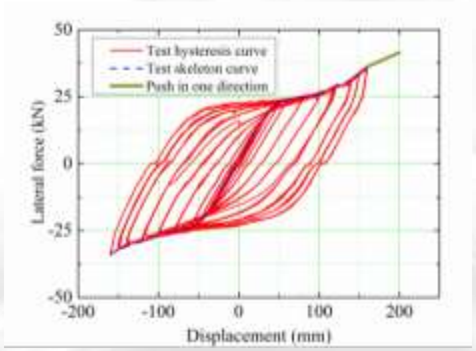


(b) hysteretic hoops

Deformation and hysteretic hoops of a TSD

- ✓ From hysteretic hoops, it can be see that TSD has a good energy dissipation capacity

# 3 Energy dissipation for of long span cable-stayed bridges

# 3 Energy dissipation for of long span cable-stayed bridges

(a) Deck-bent2 connection

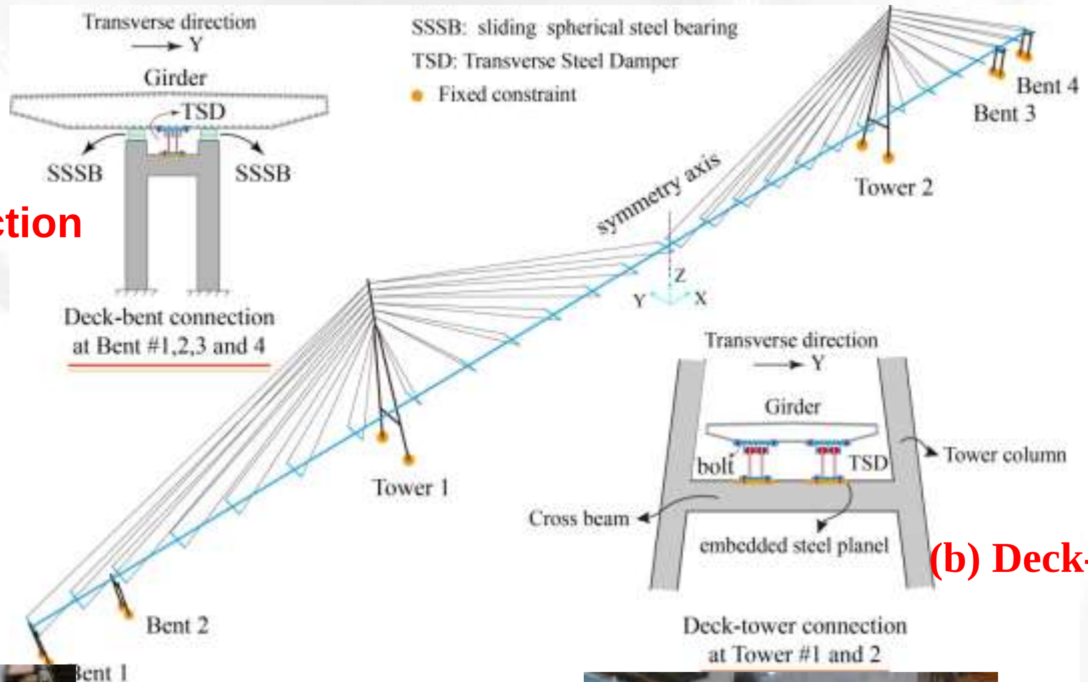


(b) Deck-tower2 connection



Figure 4. Configurations of TSDSS

Figure 5. TSDSS photographs: TSDs installed at deck-bent/tower connections

# 3 Energy dissipation for of long span cable-stayed bridges

## Test cases

- The three test case, name as TSDSS1, TSDSS2 and TFS for the comparisons of deck-bent and deck-tower connections are carried out.
- For comparison, the conventional TFS was also tested, in which fix constraints were applied at all deck-bent and deck-tower connections in the transverse direction.

Table 2. The deck-bent/tower connections for three test cases

| Direction | system | Deck-bent/tower connection | |
|---|---|---|---|
| | | Bent #1, 2, 3 and 4 | Tower #1 and 2 |
| Transverse | TSDSS1 | one TSD-1+two SSSBs | two TSD-1s |
| | TSDSS2 | one TSD-2+two SSSBs | two TSD-2s |
| | TFS | Fixed | Fixed |
| Longitudinal | TSDSS1,TSDSS2,TFS | Moveable | Moveable |

Note: SSSB = sliding spherical steel bearing

# 3 Energy dissipation for of long span cable-stayed bridges

**Table 3. Parameters of one TSD**

| | Yield strength kN | Equivalent stiffness kN/m | Hardening ratio |
|---|---|---|---|
| TSD-1 | 0.74 | 73 | 0.185 |
| TSD-2 | 0.54 | 69 | 0.155 |

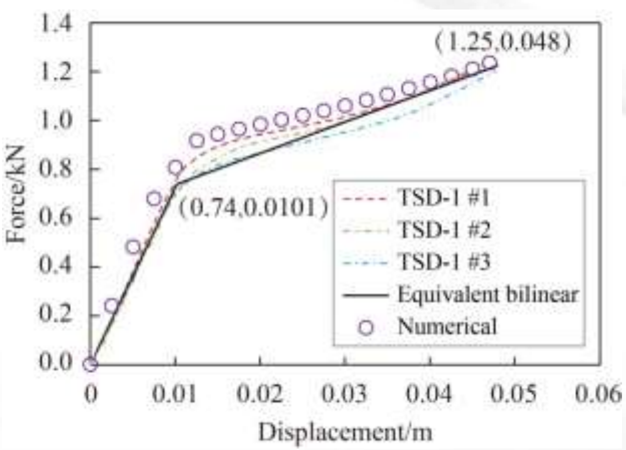


(a) TSD-1

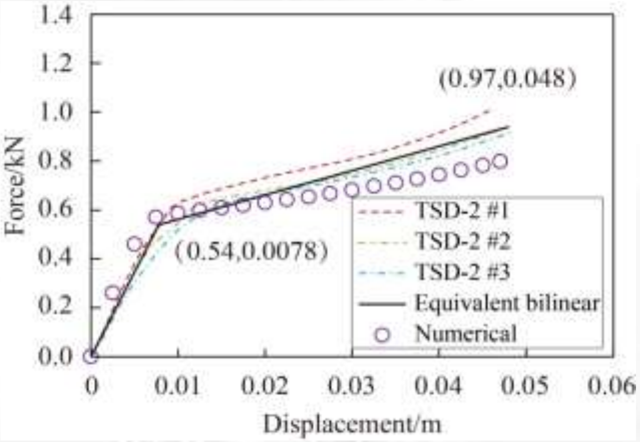


(b) TSD-2

**Figure 9. Force-displacement relationships of TSDs**

# 3 Energy dissipation for of long span cable-stayed bridges

✓ **Shake table test**

# 3 Energy dissipation for of long span cable-stayed bridges

## ◻ Test Results

- Horizontal transverse forces are measured by tri-axial-force sensors placed at the base of TSDs and bearings
- In average, compared with the conventional TFS, the peak transverse force demands are reduced by 74%, 84% and 85% at the connections of deck-Bent 1, deck-Bent 2 and deck-Tower 1, respectively.

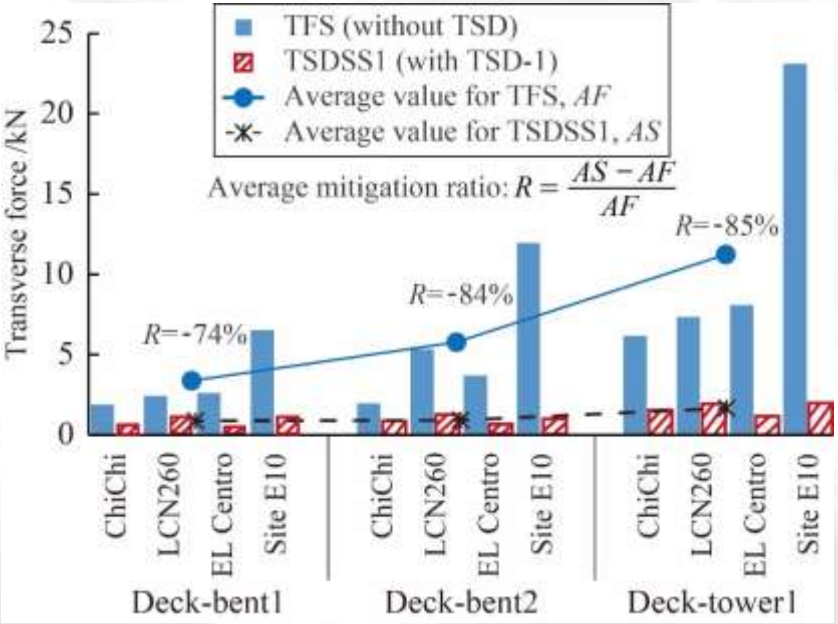


Figure 14. Comparisons of peak transverse forces at deck-bent/tower connections between the TSDSS1 and TFS under different ground motions with PGA = 0.5g

# 3 Energy dissipation for of long span cable-stayed bridges

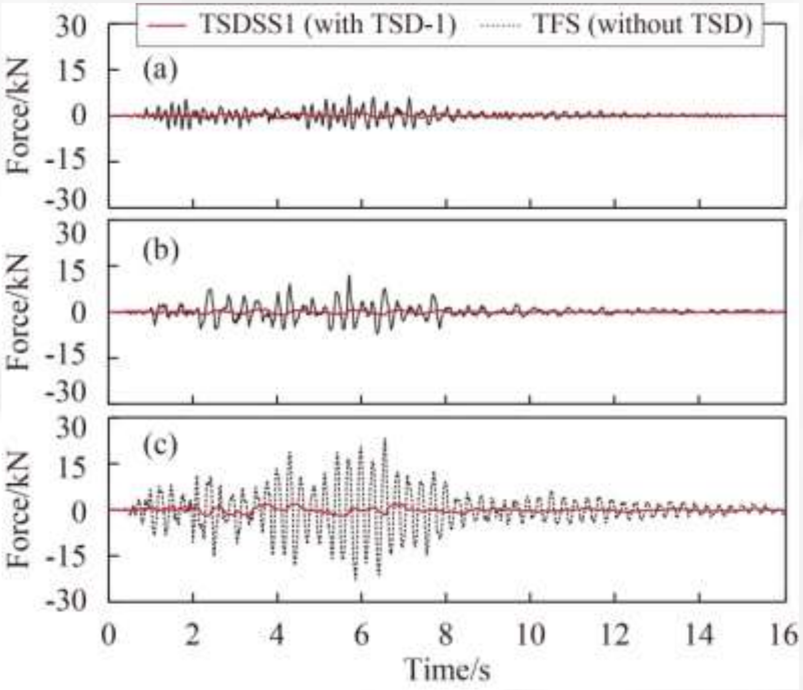


Figure 15. Transverse force time-histories at the connections of different system under **site artificial wave** : (a) deck-Bent 1 connection, (b) deck-Bent 2 connection, and (c) deck-Tower 1 connection

- **The TSDSS can significantly reduce the forces transferred from deck to bents and towers compared with the TFS. Consequently, this will reduce the seismic demands at the substructures and towers.**

# 3 Energy dissipation for of long span cable-stayed bridges

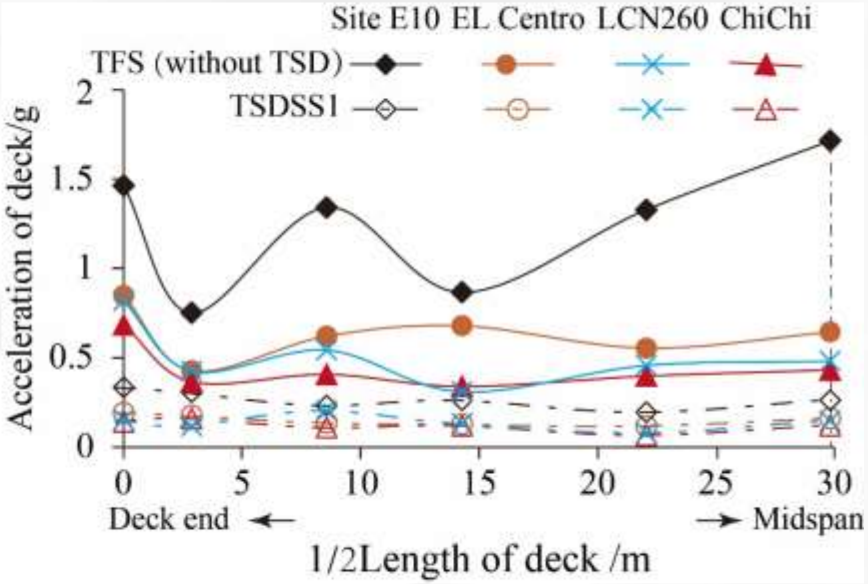


**Figure 16. Comparisons of peak transverse-acceleration along deck between the TSDSS1 and TFS under different ground motions with a PGA of 0.5g**

- **The peak transverse-acceleration of the deck in TSDSS is significantly lower than that of the TFS, which results in the remarkable decrease of the horizontal forces transferred from the deck to substructures and towers in the TSDSS**

# 3 Energy dissipation for of long span cable-stayed bridges

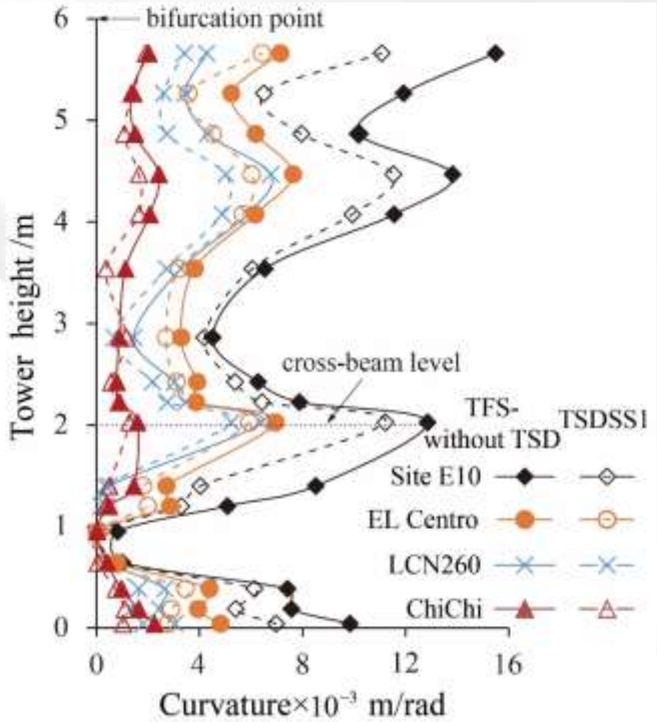


**Figure 19. Comparisons of peak curvatures along tower shaft between the TSDSS1 and TFS under**

- **TSDSS can reduce the section curvature along the tower column under near- and far-fault ground motions.**

- **Taking curvature demands at tower-bottom and pylon section above crossbeam as examples, compared with the conventional TFS, these peak curvature demands of TSDSS1 are averagely reduced by 41.7%, and 16.6%, respectively, under the four ground motions.**

# 3 Energy dissipation for of long span cable-stayed bridges

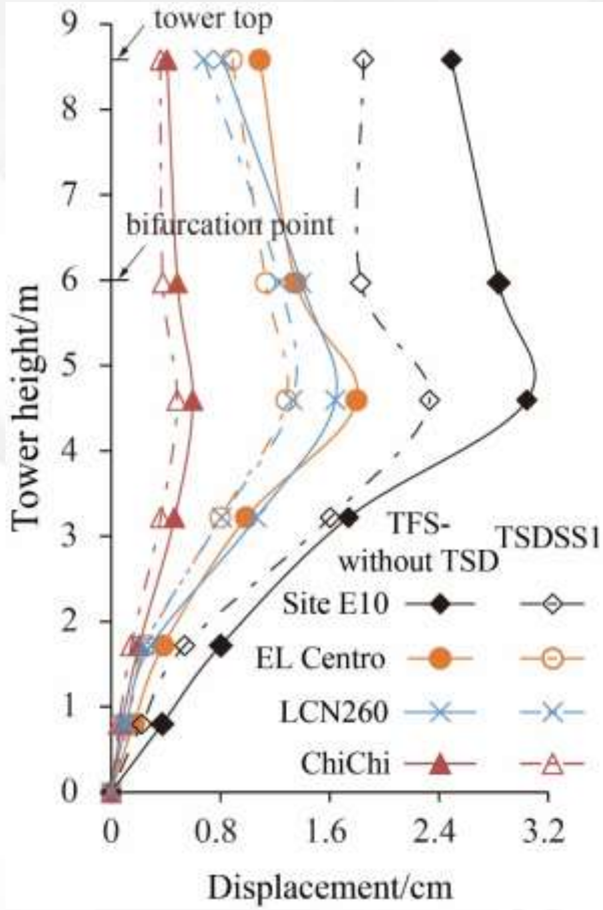


**Figure 18. Comparisons of peak transverse displacements along the tower shaft between the TSDSS1 and TFS under different ground motions with PGA = 0.5g**

# 5. Conclusion

- The numerical analyses, quasi-static model tests and shake table model test are conducted to investigate failure model of a long-span cable-stayed bridge under transverse earthquakes
- The result show that failure occurred in the upper tower column (just above cross beam) and caused significant tilt of the tower.
- The failure mode was quite consistent with the numerical simulation, quasi-static model tests and shake table model test
- However in future study, Quantitative definition of structural damage states for different levels of earthquakes which connects the performance objectives with the damage state is one of the critical problems in seismic design of a long span bridge.

# 5. Conclusion

- **The additional viscous dampers could effectively reduce the seismic responses in terms of displacements at the tower tops and deck ends and steel strain at the base of the towers under uniform excitations.**

- **However, for a long-span cable-stayed bridge, low or even negative mitigation effect might be induced by the additional viscous dampers under near-field ground motions when considering wave passage effect.**

- **Compared with the TFS, TSD can effectively reduce transverse force demands at deck-bent and deck-tower connections, and decrease lateral displacement and curvature demands along tower shafts.**

# Thank you!


Email：Lijianzh@tongji.edu.cn